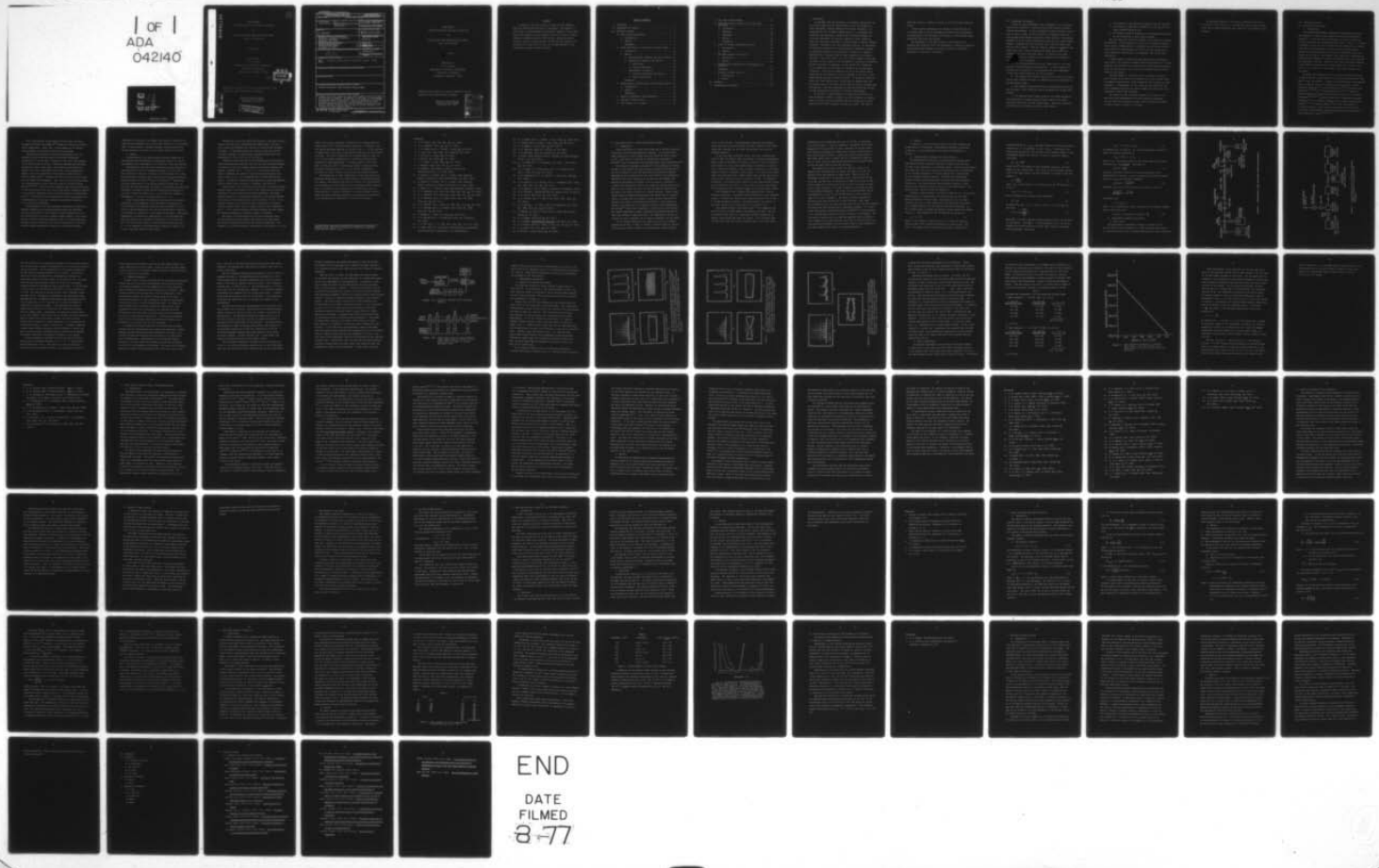
AD-A042 140 MINNESOTA UNIV MINNEAPOLIS DEPT OF ELECTRICAL ENGIN--ETC F/G 20/5
INFRARED DETECTORS AND LASER TECHNOLOGY.(U)
AUG 75 R J COLLINS N00014-68-A-0141-0002

UNCLASSIFIED NL

| OF |
ADA
042140



END

DATE
FILMED
8-77

AD A042140

(15)

FINAL REPORT

"Infrared Detectors and Laser Technology"

for

Project Grant ONR #N00014-68-A-0141-0002

Reg. No. NR 016-102

August 1975

Submitted by

R. J. Collins

Department of Electrical Engineering

University of Minnesota

Minneapolis, Minnesota 55455

DDC
RECEIVED
JUL 28 1977
E

Reproduction in whole or in part is permitted for any purpose of the United States Government.

Office of Naval Research
800 North Quincy Street
Arlington, VA 22217

DISTRIBUTION STATEMENT A
Approved for public release;
Distribution Unlimited

DDC FILE COPY

Unclassified

SECURITY CLASSIFICATION OF THIS PAGE (When Data Entered)

REPORT DOCUMENTATION PAGE		READ INSTRUCTIONS BEFORE COMPLETING FORM
1. REPORT NUMBER	2. GOVT ACCESSION NO.	3. RECIPIENT'S CATALOG NUMBER (9)
4. TITLE (and Subtitle) (6) FINAL REPORT - "Infrared Detectors and Laser Technology"		5. TYPE OF REPORT & PERIOD COVERED Final Report. - 1968-1975.
		6. PERFORMING ORG. REPORT NUMBER
7. AUTHOR(s) (10) R. J. Collins		8. CONTRACT OR GRANT NUMBER(s) (15) #N00014-68-A-0141-0002
9. PERFORMING ORGANIZATION NAME AND ADDRESS Department of Electrical Engineering University of Minnesota Minneapolis, MN 55455		10. PROGRAM ELEMENT, PROJECT, TASK AREA & WORK UNIT NUMBERS NR 016-102
11. CONTROLLING OFFICE NAME AND ADDRESS Office of Naval Research 800 North Quincy Street Arlington, VA 22217 (11)		12. REPORT DATE August 1975
		13. NUMBER OF PAGES 80
14. MONITORING AGENCY NAME & ADDRESS(If different from Controlling Office) (12) 87p.		15. SECURITY CLASS. (of this report) Unclassified
		15a. DECLASSIFICATION/DOWNGRADING SCHEDULE

16. DISTRIBUTION STATEMENT (of this Report)

Reproc APPROVED FOR PUBLIC RELEASE: DISTRIBUTION UNLIMITED of the Unitec

17. DISTRIBUTION STATEMENT (of the abstract entered in Block 20, if different from Report)

18. SUPPLEMENTARY NOTES

19. KEY WORDS (Continue on reverse side if necessary and identify by block number)

infrared photocathode, laser technology, Project THEMIS

20. ABSTRACT (Continue on reverse side if necessary and identify by block number)

A summary of the work carried out under Project THEMIS as ONR Grant #N00014-68-A-0141-0002 is presented. The emphasis in this report is the management and personnel aspects of the project. Only brief summaries of the research activities on the S-1 photosurface, self-mode locking of He-Ne lasers, optically-induced gratings, noise in optical mixing, and the optical properties of proustite are given since the work has already appeared in the literature and other technical reports.

DD FORM 1 JAN 73 1473 EDITION OF 1 NOV 65 IS OBSOLETE S/N 0102-014-6601

Unclassified

SECURITY CLASSIFICATION OF THIS PAGE (When Data Entered)

233 520

FINAL REPORT

"Infrared Detectors and Laser Technology"

for

Project Grant ONR #N00014-68-A-0141-0002

Reg. No. NR 016-102

[illegible]st 1975

Submitted by

R. J. Collins

Department of Electrical Engineering

University of Minnesota

Minneapolis, Minnesota 55455

Reproduction in whole or in part is permitted for any purpose of the United States Government.

Office of Naval Research
800 North Quincy Street
Arlington, VA 22217

ACCESSION for
NTIS White Section
DDC Buff Section
UNANNOUNCED
JUSTIFICATION
BY
DISTRIBUTION/AVAILABILITY CODES
Dist. AVAIL. and/or SPECIAL
A

ABSTRACT

A summary of the work carried out under Project THEMIS as ONR Grant #N00014-68-A-0141-0002 is presented. The emphasis in this report is the management and personnel aspects of the project. Only brief summaries of the research activities on the S-1 photosurface, self-mode locking of He-Ne lasers, optically-induced gratings, noise in optical mixing, and the optical properties of proustite are given since the work has already appeared in the literature and other technical reports.

Table of Contents

I. Background 1

II. Management and Summary 3

III. Technical Program 6

A. The Ag-O-Cs Photosurface 6

1. Introduction 6

2. Results 8

References 11

B. Pulse Velocities in "Locked and Unlocked" Lasers . . 13

1. Introduction 13

2. Results 16

a. Intermode Beat Frequency and Group Velocity 16

b. Experimental Apparatus and Results 18

1) He-Ne Laser 18

2) Measuring Apparatus 22

c. Measurements and Results 26

1) Measuring Procedures and Results 26

2) Error Consideration 30

References 35

C. Phase Relation between Modes in Self-Locked Lasers . 36

1. Introduction 36

2. Results 41

References 45

D. Theory of Ultrashort Pulse Generation 48

E. Analysis of Mode Locking 50

F. Gain Studies in CO_2 Lasers 52

G. CO_2 Laser Plasma Studies 53

H. Mass Spectroscopic Studies of CO_2 TEA Laser Discharge 54

1. Introduction 54

2. Apparatus 54

3. Experiment 55

4. Results 56

References 58

I. Noise in Optical Heterodyne Detection 59

1. Introduction 59

2. Results 61

J. The Raman Spectra of Proustite 65

1. Introduction 65

2. Results 66

K. The Nonlinear Susceptibility and Dispersion of Proustite 71

References 72

L. Optically Induced Gratings 73

1. Introduction 73

2. Results 75

IV. Personnel 78

V. Theses/Reports Published 79

I. Background

In September 1968 the University of Minnesota applied for and was granted under Project Themis funds to carry out research on laser technology, infrared detectors and signal processing. As announced the goal of Project Themis was to "... strengthen the scientific and engineering capabilities of selected academic institutions throughout the country, enabling a larger number to carry out high-quality research in areas related to national defense problems". Building on the then developing faculty, the Department of Electrical Engineering at the University of Minnesota proposed to participate and use this opportunity to develop its research capabilities in selected areas of laser technology and infrared detectors. This final report will give a brief summary of the work, the impact of the program on the Department of Electrical Engineering and the University of Minnesota, and the effect the program has had as viewed from the University of Minnesota on the Department of Defense. The principal emphasis will be on the latter points since most of the technical data have appeared in the form of published papers, special reports and theses. It should be noted that before the first funding cycle of the grant it became clear that the funding level of the grant and the scope initially proposed were inconsistent. With the concurrence of ONR the project was limited to laser technology and studies of infrared photocathodes.

In the area of laser technology studies were carried out on mode competition effects in lasers, CO_2 laser plasmas, ring lasers, noise in optical mixing experiments and the interaction of laser radiation with weakly adsorbing liquids and solids. The area of

noise was limited to studies of mixing in the 10.6 micron radiation region.

A major problem undertaken with respect to photocathodes was a detailed study of the S1 photoemissive surface using the developing technology at the University of Minnesota of low electron energy diffraction and Auger spectroscopy.

The management of the Themis Grant at the University of Minnesota was conducted within the Department of Electrical Engineering and funds were expended on projects principally within the Department of Electrical Engineering.

II. Management and Summary

During the period September 1968 to September 1973 nine senior faculty were involved in directing thesis level research students under project Themis. To aid the purpose of project Themis a policy used in the E.E. Dept. of the University of Minnesota called for only minimum cross charging of senior tenured faculty. This charge amounted to 5% per thesis student during the year and a month summer support. Although nine were involved local "thinning" meant four had only brief support. From the efforts, however, 13 students completed their Ph.D. work and derived the major portion of their support during their work from Themis. In addition five other students received M.S. degrees, and an additional five others received a fraction of support.

Of the 13 students completing Ph.D. thesis work it is a fair question "Did DoD programs or DoD benefit?" A partial answer can be given by an accounting of the graduates and their employment. To deal with those completing the Ph.D. program:

1. One graduate has played a major role in the Air Force high energy laser program and later the adaptive optics in-house work at the Kirtland Air Base.

2. One graduate developed and used the calorimeters both high and low power, built at NBS and used as standards for the DoD laser program.

3. One graduate spent several years at Los Alamos Scientific Lab establishing a surface analysis system based on low energy electron diffraction and Auger spectroscopy. The Auger techniques were developed at Minnesota partially under Themis.

4. One graduate is now employed at Hughes in the CO_2 program.
5. One graduate is employed at Honeywell in the CO_2 and ring laser programs funded by DoD.
6. One graduate works at Livermore in the engineering division on the diagnostics of laser fusion plasmas.

The list shows that half the graduates work directly in current DoD problems. Of the remaining 7, one is in a university position, one in optical communications at Lockheed, one directs the electro optics effort in communications at IT&T (Virginia), three are in local industrial laboratories: 3M, Honeywell, and Control Data Corporation.

A large number of papers were published setting the stage or early work on CO_2 discharge plasmas; definitive studies on S-1 photo cathodes; new techniques for laser-solid or laser-liquid interaction; noise in optical mixing; mode locking and related effect in He-Ne He-Cd and CO_2 lasers.

The advantages to a university and the country at large of block funding is the ability to undertake long range research were the results cannot be well enough defined to allow writing one year proposals. A disadvantage is that trust must be placed with the local management and that the project leader must resist the local pressures to cover "weak programs".

One caution for DoD in future programs is to insist on an early and clear understanding with the university management, not only with the investigator, about policy matters and funding of faculty beyond the term of the grant.

An additional benefit of DoD from our Themis was the use of our faculty in DoD affairs e.g. the DoD high energy laser program; night vision related problems; and interaction in electrical noise effects.

III. Technical Program

A. The Ag-O-Cs Photosurface

1. Introduction

The Ag-O-Cs photocathode (commercially designated as the "S-1" photocathode) is rather unique among the practical photoemissive materials. It was the first photocathode with useful sensitivity in the visible and near-infrared spectral regions ($400nm < \lambda > 1400nm$). It appears to possess a more complex chemical composition and structure than do polycrystalline and single crystal semiconducting photoemissive materials such as the alkali antimonides, III-V compounds, and Si and Ge. And further, after extensive investigations, the mechanisms responsible for its photoelectric sensitivity had not been adequately resolved. Results of this study have been reported in the special technical report issued August 1973 by Rush. As a result, only a summary is given below. For further details, see the report.

Following the development of the Ag-O-Cs photocathode surface in 1928 by Koller[1] a large number of analytical techniques have been used to study the system. In addition to photoelectric yield measurements, a partial list of the properties and techniques includes: thermionic emission,[2-17] optical absorption,[4,17-21] electrical conductivity,[4,7,13,15-17,22] photoconductivity,[12,20,23] secondary electron emission,[24] energy and angular distribution of the photoelectrons,[12,20,25-27] structural analysis by transmission electron microscopy,[4,31] and chemical analysis using a quartz crystal microbalance,[10,11,32] flame photometry,[13] and x-ray diffraction.[33] In addition several other investigations have dealt solely with the effect of photocathode formation conditions and composition on the photoelectric yield.[4,9-11,34-37]

The investigations through about 1967 have been critically reviewed by Heimann[9] and Sommer,[38,39] making an additional detailed review superfluous. Hence, only a brief summary of the results and conclusions of the earlier work will be presented.

Fabrication techniques for Ag-O-Cs photocathodes vary considerably but most have consisted of three basic processes: preparation of a silver base, oxidation of the silver, and exposure of the silver oxide to cesium. Acceptable cathodes have been made starting with pure silver sheet, other metals electrochemically coated with silver, evaporated silver films (semi-transparent or opaque), and silver deposited by the chemical process used for silvering Dewar flasks. Oxidation has been carried out using either ac or dc oxygen glow discharges. Next, with the silver oxide usually into vacuum through low work function areas on the cesium oxide surface.[36,38,20] It has also been suggested that electron excitation in the silver-cesium oxide and cesium oxide-vacuum interfacial regions in the dominant mechanism causing the broad maximum in photoelectric yield.[27] This diversity of interpretation reflects the present lack of understanding of the long wavelength photoemission mechanism of the Ag-O-Cs photocathodes.

The dependence of the long wavelength photoelectric sensitivity chemical composition of the photocathode surface was discussed initially by Koller[34] in 1930; however, direct examination of surface characteristics has only recently become feasible. With availability of Auger electron spectroscopy (AES) as a surface-sensitive, elemental analysis technique, the direct investigation of the relationship between photoelectric sensitivity and surface chemical

composition is possible. For example, by detecting characteristic Auger electron emission from a solid under electron or x-ray bombardment, it was possible to identify elements (except hydrogen and helium) present in the outer 5 to 15 atomic layers of the solid.

2. Results

The photoelectric and Auger electron emission properties of photocathodes with well-defined configuration relating to the S-1 photocathode were investigated in an ultra-high vacuum environment.

Photoelectric yield and energy distributions were measured on cesiated silver films with thicknesses between 170 Å and 3900 Å. The variation of yield as a function of film thickness was in very good qualitative agreement with earlier optical absorption measurements by Sennett and Scott,[40] Faust,[41] and Philip.[42] Energy distribution measurements of the emitted electrons showed that, as the film thickness decreased, the number of high energy photoelectrons decreased, the number of high energy photoelectrons decreased by less than a factor of three for $h\nu > 3.5$ eV while an increase of approximately a factor of two occurred for $h\nu < 3$ eV.

Using a simple model to determine the effect of hot electron scattering on the dependence of the EDC shape and magnitude on film thickness, the observed variations were attributed to variations in optical absorption, and, for the thinnest film, variation in the density of states due to the formation procedure. From these experimental and theoretical observations, it was concluded that optically active silver islands with dimensions on the order of 100 - 200 Å would emit numbers of high energy photoelectrons for $h\nu > 3.5$ eV appeared to be significantly (possibly a factor of 10 or more) less than those for bulk silver.

Photoelectric yield and energy distributions, and Auger electron emission spectra from a polycrystalline copper sample and thick silver films were measured as a function of cesium oxide overlayer thickness. It was observed that the inelastic mean free path of the Auger electrons in cesium oxide increased exponentially from approximately 4 Å at 110 eV to 13 Å at 930 eV.

Inferring a mean free path for the photoelectron scattering in cesium oxide was more difficult than for the Auger electrons because attenuation of both the incident photons and excited electrons was present. However, for $h\nu > 3$ eV, 12 - 15 Å of cesium oxide was found to attenuate the number of high energy photoelectrons by at least a factor of 14 - 16 as compared with a cesium overlayer by itself. In addition, significant photoelectron emission was observed from the cesium oxide overlayer of thickness less than 20 Å.

Photoelectric yield and energy distributions, and Auger electron emission spectra were measured from "thick" cesium oxide films after a variety of Silver depositions and heat treatments. The photoelectric yield of the cesium oxide consisted of two contact regions, the origins of which were modified using the EDC's. For $h\nu > 3$ eV, electron emission from the cesium oxide valence band is constant although emission from a band of surface states is also detectable. For $h\nu < 3$ eV, electron emission from both surfaces and bulk states, with energies extending to the Fermi energy, is present.

The effect of silver depositions and heat treatments under various conditions allows several conclusions to be drawn about the Ag-O-Cs photocathode structure and emission mechanisms. The presence of a relative minimum in photoelectric yield near $h\nu = 3.8$ eV

results from silver particles of minimum size or greater which are within about 10 Å of the solid-vacuum interface. In addition, the high energy electrons observed in the EDC's for $h\nu > 3.5$ eV originate in these silver particles or other silver atoms near the solid-vacuum interface. An earlier conclusion that the photoelectric yield for $h\nu \gtrsim 4$ eV originates predominantly in the cesium oxide was substantiated by AES measurements. With these results, the recent work by Timan was shown to substantiate Sommer's suggestion that the unique infrared sensitivity in the Ag-O-Cs photocathode originates in silver islands very near the photocathode surface.

The possibility of other combinations of materials exhibiting comparable photoelectric yield characteristics was examined briefly. As a result, using Sennett and Scott's criterion for the existence of an increase in optical absorption with decreasing metal particle size in conjunction with measurements of photoelectric yield on planar samples, it should be possible to predict whether or not a particular metal-overlayer combination would exhibit photoelectric yield characteristics comparable to Ag-O-Cs photocathodes.

(Because these treatments deviated from commercial processing techniques the resulting photoelectric yields were lower than those obtained commer ally.)

References

1. L. R. Koller, Gen. Elec. Rev. 31, 476 (1928).
2. N. R. Campbell, Phil. Mag. 12, 173 (1931).
3. J. H. deBoer and M. C. Teves, Z. Physik 83, 521 (1933).
4. S. Asao, Proc. Phys. Math. Soc. Japan 22, 448 (1940).
5. P. Gorlich, Z. Physik 116, 704 (1940).
6. F. Eckart, Ann. Physik 16, 322 (1955).
7. J. E. Davey, J. Appl. Phys. 28, 1031 (1957).
8. W. Heimann, Phys. Stat. Sol. 6, 713 (1964).
9. W. Heimann, Final Technical Report, Contract No. DA-91-591-EUC-3510, U.S. Army (1965).
10. W. Heimann, E. Kansky, and E. L. Hoene, Final Technical Report, Contract No. DA-91-591-EUC-3890, U.S. Army (1966).
11. W. Heimann, E. Kansky, and E. L. Hoene, Final Technical Report, Contract No. DAJA 37-67-C-0492, U.S. Army (1968).
12. S. Weber, Ph. D. Thesis, Technischen Hochshule, Stuttgart (1964).
13. M. T. Pakhomov, Bull. Acad. Sci. USSR, Phys. Ser. 33, 471 (1969).
14. M. T. Pakhomov, Bull. Acad. Sci. USSR, Phys. Ser. 33, 478 (1969).
15. M. T. Pakhomov and A. E. Melamid, Bull. Acad. Sci. USSR, Phys. Ser. 35, 281 (1971).
16. M. T. Pakhomov, Bull. Acad. Sci. USSR, Phys. Ser. 35, 289 (1971).
17. M. T. Pakhomov and A. E. Melamid, Bull. Acad. Sci. USSR, Phys. Ser. 35, 562 (1971).
18. M. Sugawara, J. Phys. Soc. Japan 12, 1282 (1957).
19. A. E. Melamid and N. S. Khlebnikov, Radio Eng. Electron 9, 819 (1964).
20. K. S. Neil and C. H. B. Mee, Phys. Stat. Sol. (a) 2, 43 (1970).
21. H. Timan, paper B5, Conference on Photoelectric and Secondary Electron Emission, Minneapolis, 1971 (unpublished).

22. W. J. Harper and W. J. Choyke, J. Appl. Phys. 27, 1358 (1956).

23. S. Pakswer and W. O. Reed, J. Appl. Phys. 22, 987 (1951).

24. A. H. Sommer, J. Appl. Phys. 42, 567 (1971).

25. N. A. Soboleva, Radio Eng. Electron 4, 204 (1959).

26. N. A. Soboleva, Radio Eng. Electron 4, 223 (1959).

27. J. Burns, Final Technical Report, Contract No. DA-44-009-AMC-938(7), U.S. Army (1969).

28. A. I. Frimer and A. M. Gerasimova, Sov. Phys. - Tech. Phys. 26, 705 (1956).

29. A. I. Frimer, E. M. Belavtseva, and A. M. Gerasimova, Sov. Phys. - Tech. Phys. 26, 530 (1956).

30. L. N. Bykhoskaia and I. M. Kushnir, J. Tech. Phys. USSR 25, 2477 (1955).

31. N. A. Soboleva, A. S. Shefov, and V. N. Tolmasova, Bull. Acad. Sci. USSR, Phys. Ser. 26, 1393 (1962).

32. S. A. Bendson, M.S.E.E. Thesis, University of Minnesota, (1967).

33. W. H. McCarroll, unpublished work as quoted in Ref's 38 and 39.

34. L. R. Koller, Phys. Rev. 36, 1639 (1930).

35. C. H. Prescott and M. J. Kelly, Bell Syst. Tech. Journ. 11, 334 (1932).

36. P. G. Borziak, V. F. Bibik, and G. S. Kramerenko, Bull. Acad. Sci. USSR, Phys. Ser. 20, 939 (1956).

37. E. Kansley, B. Otrin, S. Jeric, and P. Gspan, Suppl. Nuovo Cimento 5, 139 (1967).

38. A. H. Sommer, RCA Review 28, 543 (1967).

39. A. H. Sommer, Photoemission Materials, John Wiley, NY (1968).

40. R. S. Sennett and G. D. Scott, J. Opt. Soc. Am. 40, 203 (1950).

41. R. C. Faust, Phil. Mag. 41, 1238 (1950).

42. R. Philip, J. Phys. Radium 21, 165 (1960).

B. Pulse Velocities in "Locked and Unlocked" Lasers

1. Introduction

Pulse velocities of a fully self-locked and a partially unlocked He-Ne laser have been experimentally compared. It was found that pulse velocity of a fully locked laser was larger by about 9 parts in 10^6. This result is contrary to earlier data published by Garside[1,2] but is consistent with the theoretical work of Willenbring.[3,4]

The effects of population pulsation on the propagation of laser pulses in a gain medium has been recently analyzed by Willenbring.[3,4] One of his results is that the third-order polarization sidebands generated by the interactions of the laser field with the modulating population can cause a decrease of the slope of the resonant dispersion and therefore an increase in pulse velocity. Physically, it means that population pulsation can cause the leading edge of the pulse to see a higher gain than the trailing edge and hence shifts the peak of the pulse to travel at a faster velocity. Since a self-locked laser has population modulation much larger than an unlocked laser, it follows that an increase in pulse velocity should be observed as the laser is switched from unlocked to locked operation. However, such prediction is in apparent conflict with measurements by Garside,[1,2] which show a decrease in pulse velocity with locking. This report describes in detail a measuring technique developed to check the validity of Garside's data. Our experimental results are contrary to that of Garside, but in general agreement with the theory.

In the present experiment, the laser was set up for bistable operation such that it could be locked or unlocked simply by adjusting the cavity length by means of a piezoelectric crystal mounted

on one of the mirrors. The experimental technique for comparing group velocities involved measuring the small changes in the fundamental beat frequency as the laser was switched from locked to unlocked operation.

It has long been recognized[5] that a so-called unlocked laser does not have its several modes oscillating in complete independence. Rather, some of the modes are generally coupled to form a travelling pulse within the laser, while other modes are switching on and off due to competition effects. What is usually referred to as unlocked laser is actually a partially locked laser. It is noisy, has a much lower pulse amplitude than a phase-locked laser and has large variations in the pulse amplitude as a function of time. By observing the change in fundamental beat frequency as the laser becomes locked one can determine the change in pulse velocity in the laser medium as the pulse amplitude increases and all of the modes become locked.

The fundamental beat frequency was measured using a photomultiplier detector, a heterodyne receiver-amplifier, and a frequency counter. Counting was carried out by down-converting from 136 MHz to 30 MHz followed by feeding a converter-counter unit, which in turn down converts the 30 MHz signal to less than 10 MHz.

This system has been used previously,[6,7,8] for measuring the pulse velocity of locked lasers, and performs very well. But for an unlocked laser there is a potentially serious problem due to missing counts which come about as follows. In an unlocked laser the mode amplitudes and phases fluctuate greatly, and under some

circumstances the fundamental beat note at 136 MHz, as displayed on an oscilloscope, is found to decrease in amplitude and virtually disappear for brief periods of time. Similarly the 30 MHz signal also virtually disappears at these times, and the counter fails to count during these intervals. Hence, the counter always tends to have fewer counts than it should, and it is important to keep the loss in count as low as possible by operating the "unlocked" laser so that the dead intervals are few and short.

The presence of missing counts can, however, result in an apparent beat frequency which is either too high or too low, depending on how the apparatus is being used. There are the two heterodyne converters in the systems, one to convert from 136 MHz to 30 MHz, and the other to convert the 30 MHz to less than 10 MHz. In both cases the converter can be set so that the signal is mixed with a higher frequency, or a lower frequency, to produce the beat at the observed frequency. This means that "missed counts" can be interpreted as an error in the 136 MHz signal to give either too high, or too low a frequency. The effect is easily observed by switching over from mixing with a lower frequency. When there are no missed counts, one gets the same value for the 136 MHz frequency. But when there are missing counts, discrepancy appears. It is possible that previous results reported by Garside[1,2] on pulse velocity in an unlocked laser could be in error because of this problem. For the results reported here the laser and apparatus were operated in such a manner as to insure that the error due to missing counts was not significant compared with the actual change in beat frequency as the laser changed from locked to unlocked operations.

2. Results

In section a, the relationship between the beat frequency and group velocity is discussed. Experimental apparatus is described in section b while measurements and results are presented in section c .

a. Intermode Beat Frequency and Group Velocity

The experimental techniques for measuring beats between adjacent modes has been previously employed in studying the velocity of laser pulse propagating in a resonant medium. Faxvog and Carruthers[9] have shown that the pulse velocity of mode locked laser is determined by the resonant dispersion of the gain medium and is proportional to the intermode frequency spacing. Garside[1] has compared beat spectra of both locked and unlocked ring laser with his dispersion calculation. The relationships among resonant dispersion, group velocity and intermode frequency spacing can be demonstrated in the following way, similar to that of reference 9.

Consider a laser resonator with cavity length of "L". Longitudinal modes oscillate at frequencies over which the gain of the laser medium exceeds the cavity losses. For simplicity, let the laser oscillate with 2M + 1 modes symmetrically located about the center of the Doppler profile with the central mode having frequency ω_o. For a locked laser, the modes are exactly equally spaced with separation of $\Delta\omega$. The frequency of the m^{th} mode can be written as

$$\omega_m = \omega_o + m\Delta\omega \qquad (1)$$

where m is an integral value and $-M \leq m \leq M$. When the laser becomes unlocked, the intermode spacings are no longer equal. However, if we assume that the spacings vary around a statistically

weighted average of $\langle\Delta\omega\rangle_{ave}$, the mode frequency can still be approximated by Eq. (1) by replacing $\Delta\omega$ with $\langle\Delta\omega\rangle_{ave}$. The modes of the cavity must also satisfy the condition of an integral number of half wavelengths between the mirrors. In terms of mode wave number, this means

$$k_m = k_o + \frac{m\pi}{L} \qquad (2)$$

where the m^{th} wave number is again expressed around k_o, the wave number for the central mode. As a result of the dispersive properties of the laser medium, the mode frequency is related to the wave number by

$$\omega_m = \frac{k_m c}{\eta(\omega_m)} \qquad (3)$$

Here, $\eta(\omega_m)$ is the index of the refraction for the m^{th} mode and is given by

$$\eta(\omega_m) \simeq 1 + 1/2\chi'(\omega_m) \qquad (4)$$

For the symmetric set of modes being considered

$$\omega_o = K_o c \qquad (5)$$

By subsituting Eqs. (1) (2), and (5) into Eq. (3) it is easy to show that

$$\eta(\omega_m) = \frac{1 + \frac{m\Delta\Omega}{\omega_o}}{1 + \frac{m\Delta\omega}{\omega_o}} \qquad (6)$$

where $\frac{\pi c}{L} = \Delta\Omega$ is the frequency spacing between modes in the absence of gain medium. Since $\frac{\Delta\omega}{\omega_o} << 1$, the denominator of Eq. (6) can be expanded into Taylor series and higher order terms in the series can be neglected. This gives

$$\eta(\omega_m) \simeq 1 + m(\Delta\Omega - \Delta\omega)/\omega_o \quad . \quad (7)$$

By comparing Eq. (4) with Eq. (7), the gain dispersion is seen to relate to the mode separation by

$$\chi'(\omega_m) = 2m(\Delta\Omega - \Delta\omega)/\omega_o \quad .$$

From Eq. (6), the group velocity of the locked modes can be calculated from $v_g = \frac{c}{\eta + \omega\, d\eta/d\omega}$. The result is

$$v_g(\text{lock}) = \frac{c\Delta\omega}{\Delta\Omega} \quad . \quad (8)$$

Similarly, the group velocity for the unlocked modes can be approximated by replacing $\Delta\omega$ with a statistically weighted average value of $\langle\Delta\omega\rangle_{ave}$ as previously discussed:

$$v_g(\text{unlock}) = \frac{c\langle\Delta\omega\rangle_{ave}}{\Delta\Omega} \quad . \quad (9)$$

Therefore, the ratio of the two group velocities is given by

$$\frac{v_g(\text{unlock})}{v_g(\text{lock})} = \frac{\langle\Delta\omega\rangle_{ave}}{\Delta\omega} \quad .$$

By assuming that

$$\Delta\omega = \langle\Delta\omega\rangle_{ave} + \delta$$

where δ is an experimental value, one obtains the difference between the two velocities to be

$$v_g(\text{lock}) - v_g(\text{unlock}) = v_g(\text{lock}) \cdot \frac{\delta}{\Delta\omega} \quad . \quad (10)$$

b. Experimental Apparatus and Results

1) He-Ne Laser

The experimental arrangement is shown in Figures 1 and 2. The 6328 Å He-Ne laser consisted of a He-Ne discharge tube placed in a two-mirror cavity with a methane absorption cell and an aperture.

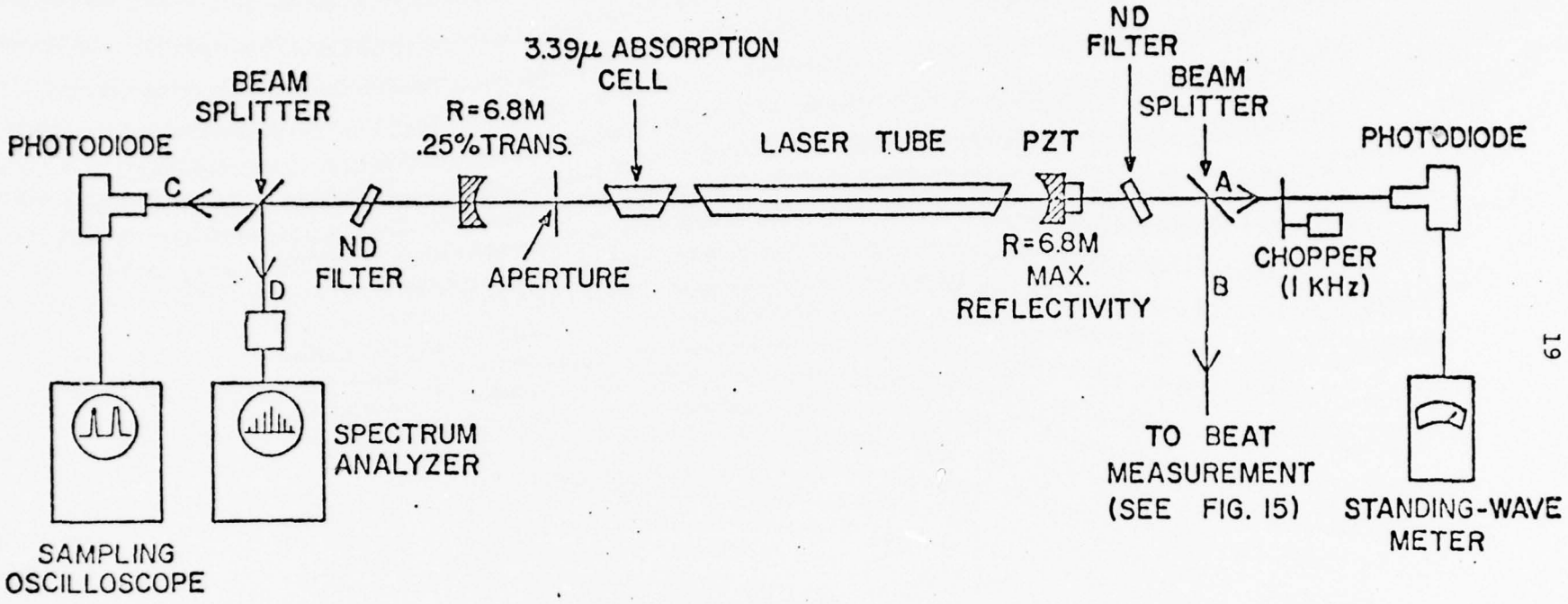


Figure 1 Experimental setup for group velocity measurement.

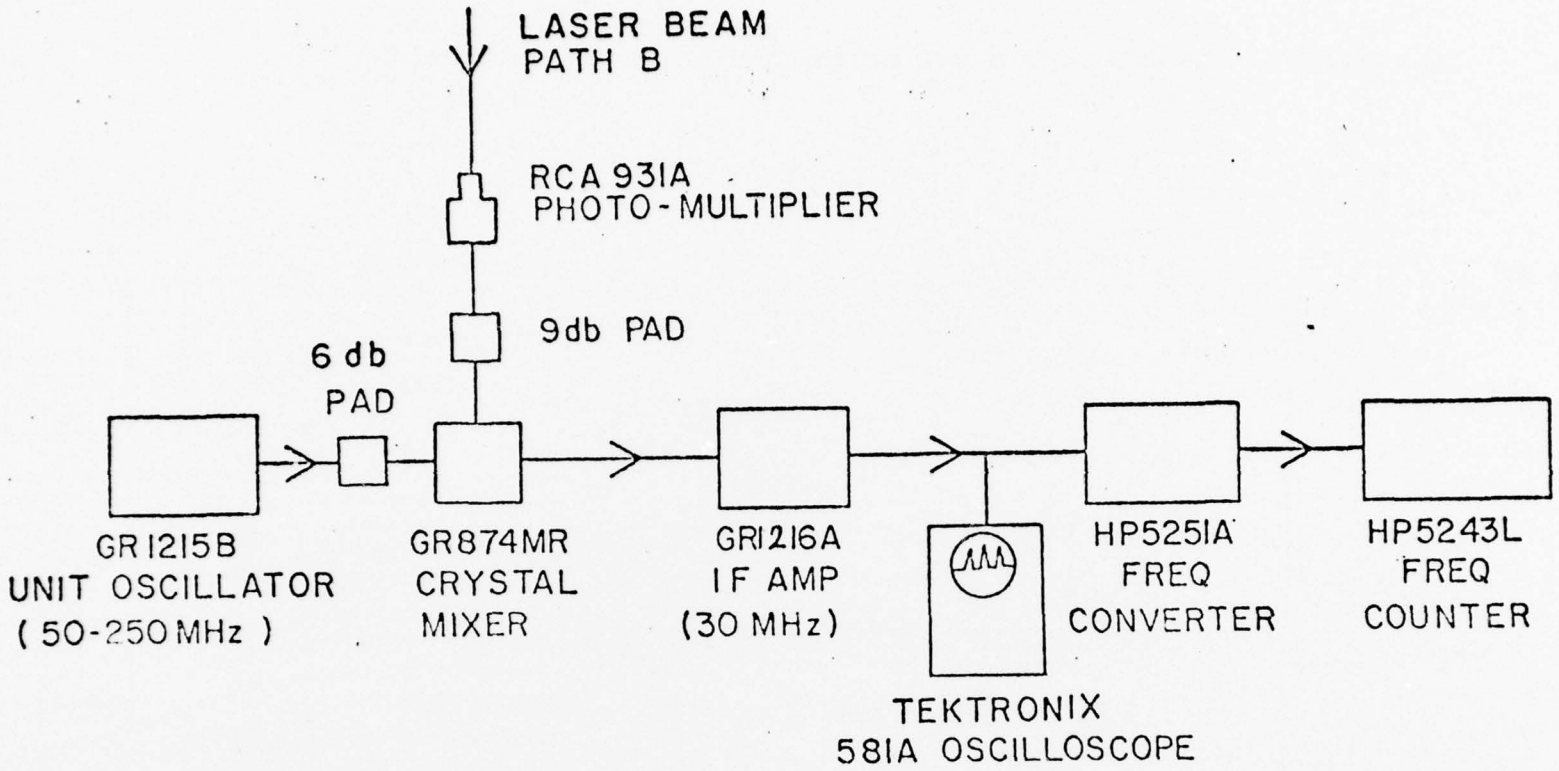


Figure 2 Block diagram of the heterodyne detection system to measure the intermode beat frequency.

The cavity was 110 cm in length and was made up of two curved mirrors, both of which had a radius of cocurvature of 6.8 m and were dielectric-coated for 6328 Å. One was specified for 0.25% power transmission and the other for maximum reflectivity ($R \simeq 99.9\%$). The high reflectivity mirror was mounted on a piezoelectric translator to allow small change of cavity length, on the order of $\lambda/2$. The laser gain tube was Pyrex capillary tubing of 2.6 mm i.d. with quartz windows oriented at the Brewster angle at both ends. It was originally filled with 10:1 gas mixture of He^3:Ne^{20} to a total pressure of 2.4 Torr. The tube was DC excited and the active discharge length was about 50 cm. Throughout the experiment, the discharge current was kept at 8 ma. To prevent simultaneous laser oscillation at the 3.39 μ transition, a 1.25" long gas cell filled with methane to atomospheric pressure was added. A variable aperture was also placed inside the cavity to insure that the laser would operate with only TEM_{00q} modes. Furthermore, the aperature could be used to vary the internal laser power without changing the laser excitation. When the aperture was sufficiently closed, the laser was self-pulsing for all positions of mode frequencies. If the aperture was sufficiently opened, it became free-running. In between, there was a region where bistable operation could be obtained, in which the laser could be locked or unlocked simply by tuning the PZT element. The present experiment was designed to operate in this region.

To avoid mechanical vibrations from the building, the whole laser system was securely fastened to a 4' x 4' x 1' granite slab which weighs about 2 tons. The slab was in turn isolated from the floor by four spring-shock mounts. Air turbulence through the

laser cavity was minimized by covering the open region between the laser components with mylar tubing. After the laser had been warmed up for an hour or so, the cavity length was found to drift less than $\lambda/10$ in a period of 20 minutes.

2) Measuring Apparatus

Figures 1 and 2 show the arrangements for the measuring apparatus. Neutral density filters were placed between the laser mirrors and the measuring apparatus so that feedbacks due to back-scatterings from the detecting surfaces could be effectively eliminated. Laser outputs from both mirrors were split into four beam paths. Path A was used to monitor the one-way internal power of the laser. The beam was chopped at 1 KHz, detected by an RCA 922 vacuum photodiode and fed into a GR 1234 standing-wave meter. The meter had been calibrated for the present setting by replacing the 0.25% transmission mirror with a calibrated 1.8% transmission mirror through which the laser power could more accurately be determined by an EG & G 560 Lite-Mike power meter. High-resolution expanded scales of the standing-wave meter also permitted attenuation indications to be resolved into 0.02 db increments.

To observe the locking condition of the laser both the mode spectrum and the time-resolved laser output were monitored. Optical frequency spectra could be observed continuously from path C by a SP Model 420 Spectrum Analyzer which consisted of a scanning confocal interferometer, a photodiode and an oscilloscope display. In path D, the laser output was measured by an HP 4203 photodiode and HP 140A - 1431A sampling oscilloscope. The speed of the combined system was limited by the photodiode which had a rise time of less

than 1 nsec but on the same order of the width of the laser pulse. Therefore, the measured wave form might be slightly wider than the actual pulse shape.

The beat frequency between adjacent modes at about 136 MHz was measured from path B. The detection system consisted of an RCA 931A photomultiplier, followed successively by a GR 874 MR crystal mixer, a GR 1216-A IF amplifier and an HP 5251A - 5243L frequency counting unit, as shown in Fig. 2. The photomultiplier is a nine-stage type with S-4 type spectral response. Its frequency response was checked to be adequate for the 136 MHz beat signal. A ground glass plate was placed in front of the detector. Its purpose was to diffuse the laser beam so as to average the response of the photocathode.

The beat signal from the photomultiplier and the signal from the GR 1215B Unit Oscillator, which was set to a frequency approximately 30 MHz below the beat signal, were mixed in the GR 874 MR crystal mixer. The difference-frequency produced was fed into a GR 1216-A 30 MHz IF amplifier and then AC coupled away before it reached the rectifying stages of the amplifier. The amplification was necessary in order to provide sufficiently large signals for the frequency counting unit which had a sensitivity of 100 mV. A HP 5251A heterodyne converter was placed ahead of the HP 5243L electronic counter. It down converted the ~ 30 MHz signal such that the difference was within the counter's range.

For the present experiment, the gate time of the counter was set at 0.1 sec and the frequency converter was on the 30 MHz scale. Also, the unit oscillator was so adjusted that the final difference

frequency appeared on the counter was between 30 KHz and 200 KHz. The purpose of this experiment was to observe the small changes of this frequency reading as the laser switched from locked to unlocked operation.

When the laser is locked, the amplitudes and relative phase of the modes are constant in time, resulting in a stable beat signal, and the beat measurement is straightforward. In contrast, as the laser becomes unlocked, the oscillating modes fluctuate randomly both in amplitudes and in phases. As previously discussed, the amplitude of the intermode beat varies in time and may even occasionally completely disappear, resulting in missing counts on the frequency counter. Figure 3(a) shows the schematic diagram of the frequency counter. The input signal is amplified and then converted into uniform pulses by the Schmitt triggering network. As is illustrated in Figure 3(b), this signal must be large enough to cross both hysteresis levels of the input Schmitt trigger before an output pulse can be produced. The pulses thus formed are routed through the time gate and into the decade counting assemblies. The number of pulses being counted in the decade counter during the open-gate interval is a measure of the average input frequency for that interval. In the event that the amplitudes of some of the beats from the unlocked laser are below the triggering level of the Schmitt circuit, missing counts occur and the frequency is in error. For this reason, beat measurement could not be performed for any arbitrary unlocked laser. Fortunately, when the laser was not badly unlocked, intensity fluctuations of the beat signal were generally small and reproducible results could be obtained. To help insure that the

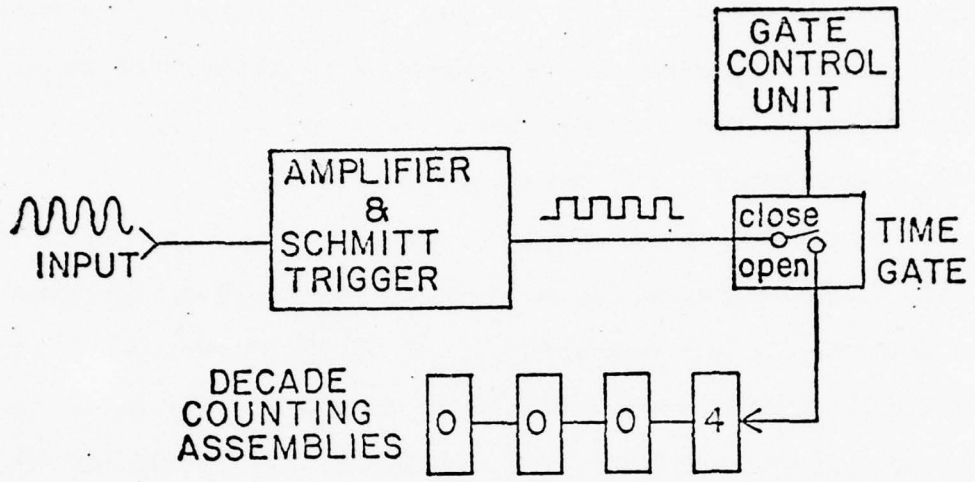


Figure 3(a) Schematic diagram of the frequency counter.

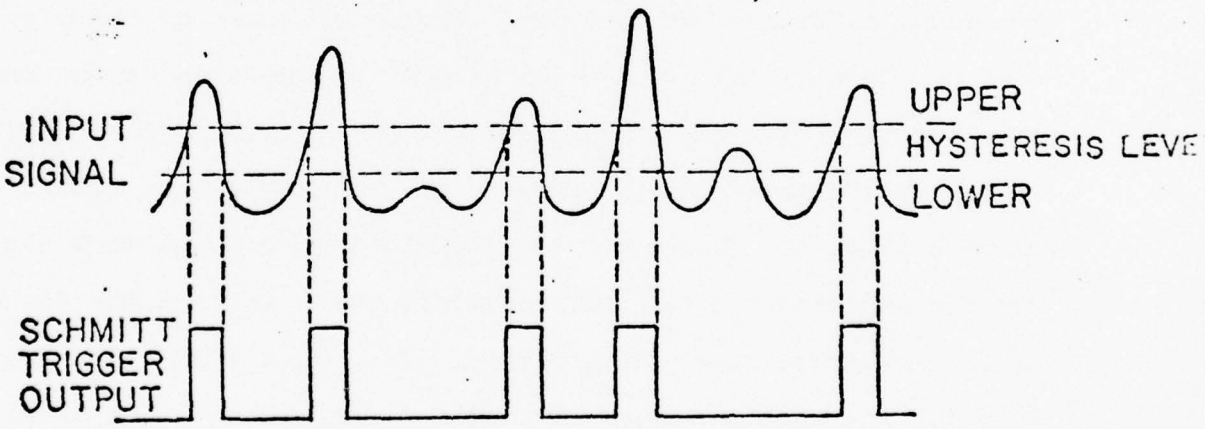


Figure 3(b) Input signal must be large enough to cross both hysteresis levels of the input Schmitt trigger to produce an output count.

missing counts could be held to an insignificant level part of the output from the IF amplifier was fed to a Tektronix 581A oscilloscope as a monitor. Experimental procedures for making such measurement are discussed in the next section.

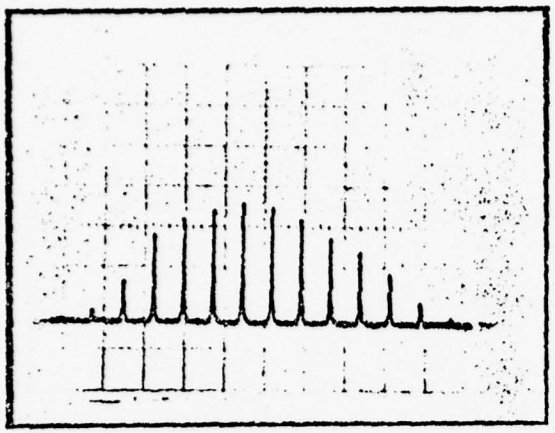
c. Measurements and Results

1) Measuring procedures and results

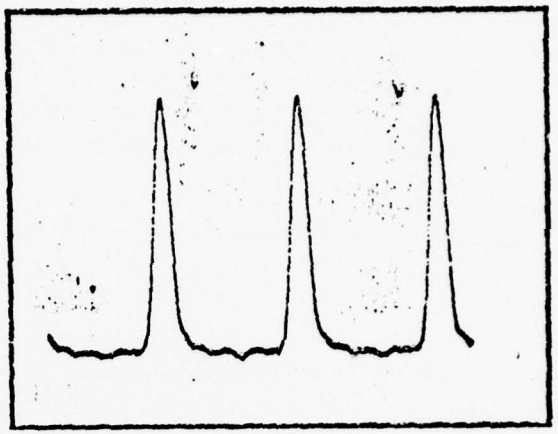
The laser was adjusted to have a one-way internal power of about 290 nW. It was operated in the bistable region in which the laser could be locked or unlocked by tuning the PZT element mounted on one of the end mirrors. The oscillating conditions of the laser are illustrated in Figures (4) - (6).

Figures 4(a) and 4(b) show respectively the mode spectrum and pulse output of the laser when it was self-locked. The 30 MHz down-converted beat signals as monitored by the Tektronix 581A oscilloscope are shown in Figs. 4(c) and (d). The intensities of the signal were constant in time and there were no ambiguities on the beat measurements. As the PZT element was moved about $\lambda/20$ (optical frequency change of about 14 MHz), the laser began to unlock as shown in Fig. 5. These records clearly show how the mode amplitudes and the amplitude of the beat note fluctuate in time for the unlocked laser. However, there were periods [Fig. 5 (d)] when the beat signals were stable enough so that measurement could be obtained. Although the laser output still exhibited periodical pulsed waveform, the pulse amplitude was observed to be about 15% less than that for the locked laser.

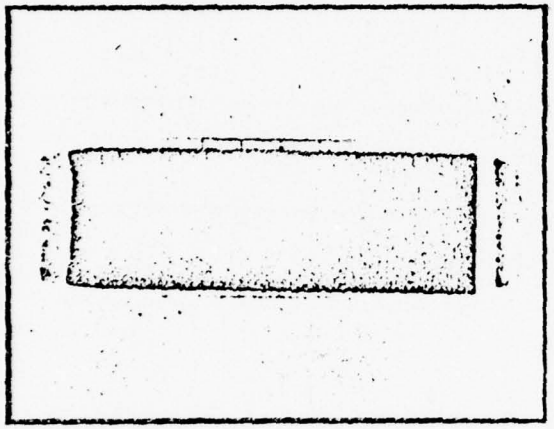
As the laser was further tuned to higher mode frequencies, it became free-running as shown in Fig. 6. The beat signal fluctuated



(a)

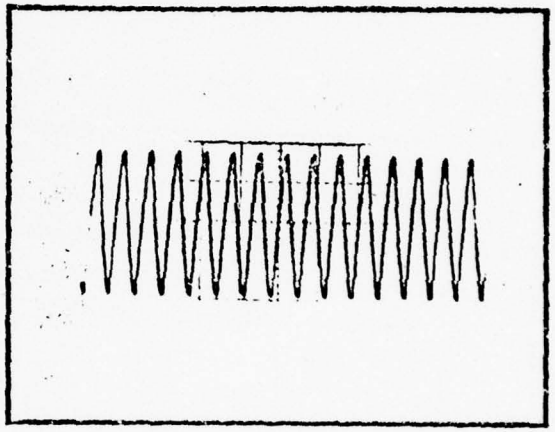


(b)



Horizontal scale = 20μsec/div

(c)



Horizontal scale = 0.05μsec/div

(d)

Figure 4 (a) Optical mode spectrum of the laser when it is self-locked. The intermode spacing is 136 MHz. (b) Corresponding output of the self-locked laser. Time between pulses is about 7.3 nsec. (c) and (d) Intensity stabilities of the intermode beat signal of the self-locked laser. Vertical scale = 100 mV/div.

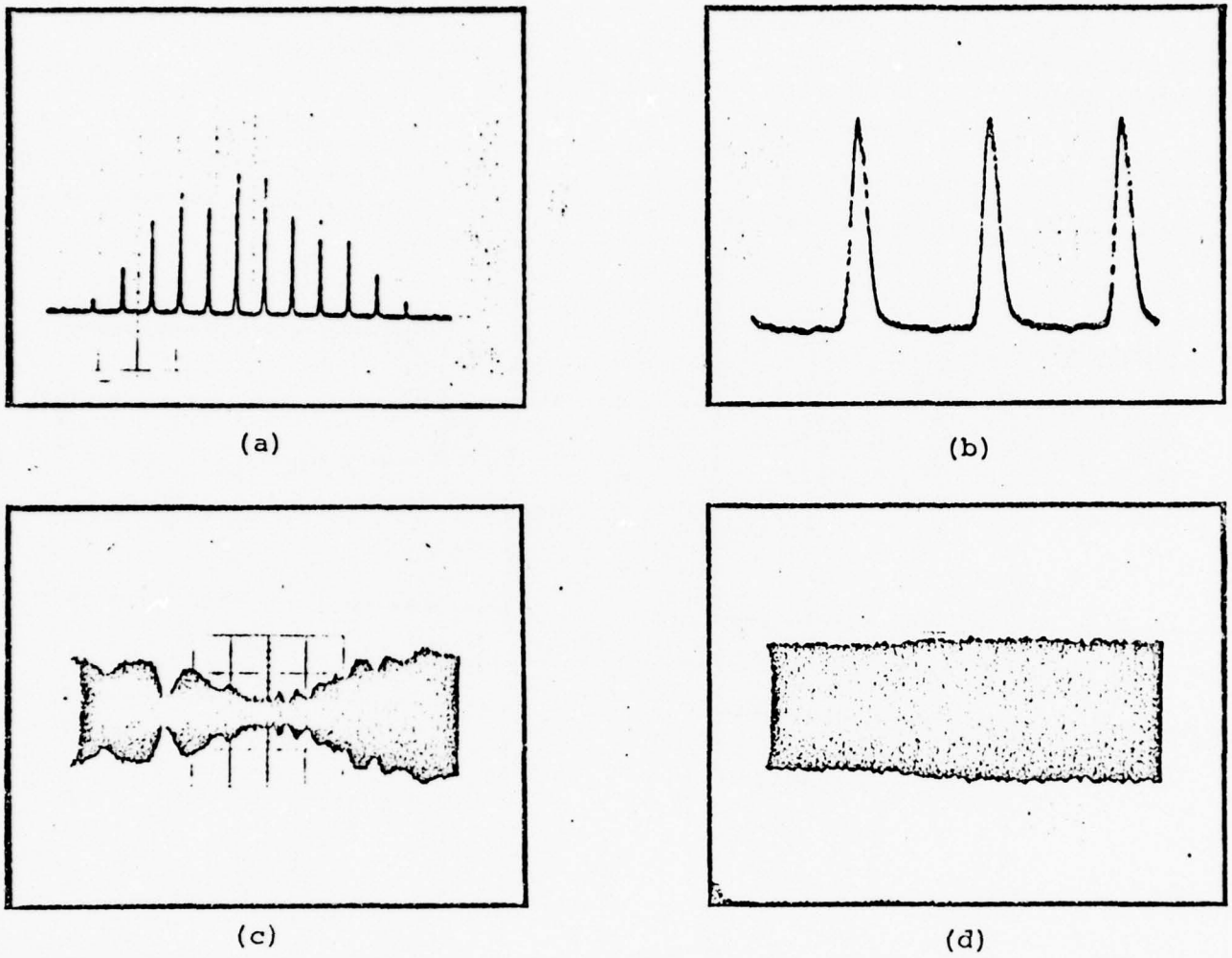


Figure 5 (a) Optical mode spectrum of the laser when it is not badly unlocked. The intermode spacing is 136 MHz. (b) The corresponding laser output. (c) and (d) Intensity stabilities of the intermode beat signal. Horizontal scale = 20 μsec/div. Vertical scale = 100 mV/div.

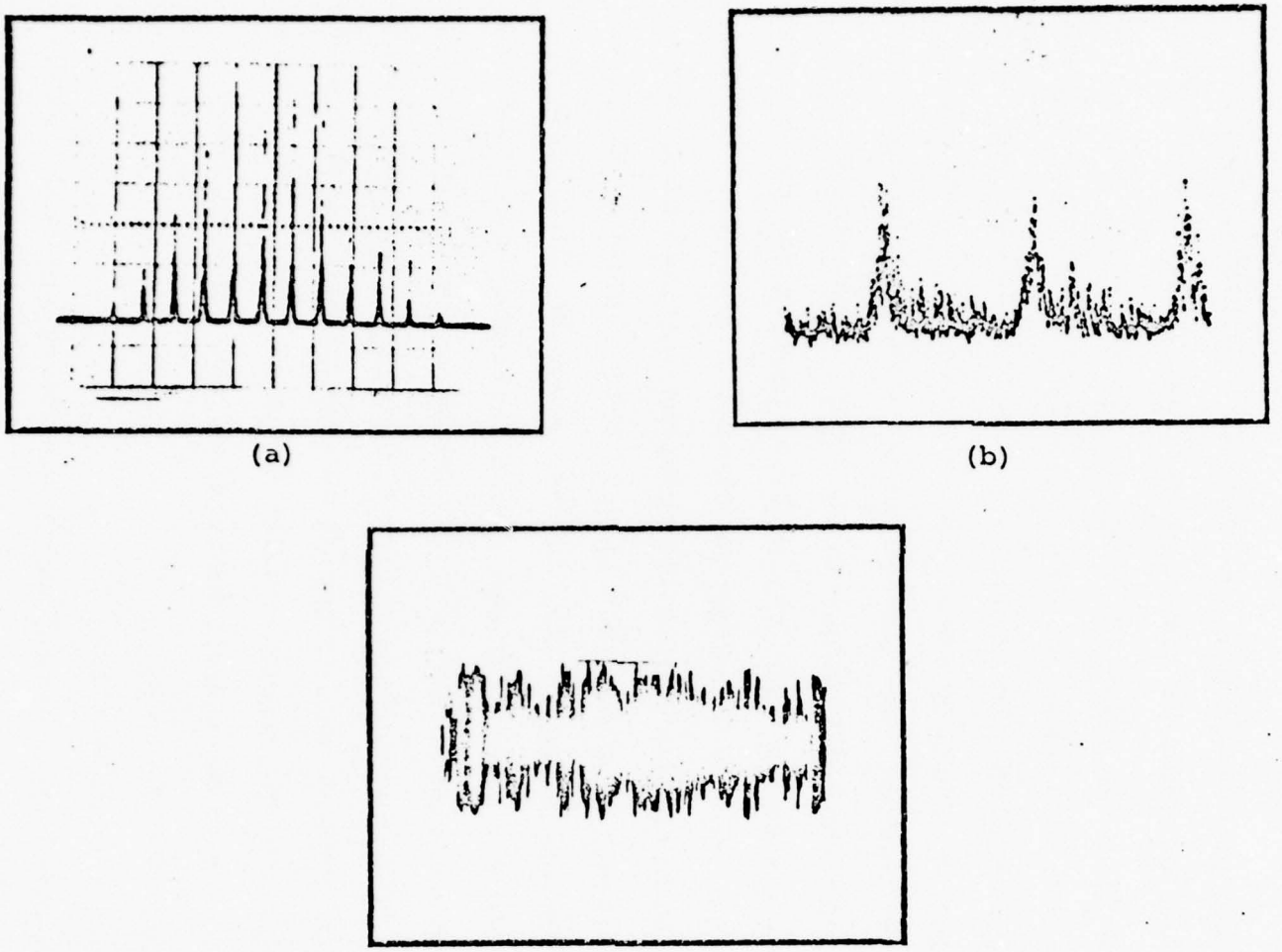


Figure6 9 (a) Optical mode spectrum of a badly unlocked laser. Intermode spacing is 136 MHz. (b) Corresponding laser output. (c) Intensity fluctuations of the intermode beat signal of the unlocked laser. Horizontal scale = 20 μsec/div. Vertical scale = 100 mV/div.

so badly that consistent measurement was not possible. Therefore, the present experiment was restricted to compare beat measurements between locked and not-so-badly-unlocked lasers as represented in Figs. (4) and (5).

Measuring procedures were as follows: (1) First, the unit oscillator was adjusted so that the beat signal from the IF amplifier (normally 30 MHz) was actually 30 KHz to 200 KHz above 30 MHz. The PZT element was then tuned to provide stable self-locking and the frequency reading from the counter was recorded. Next, the cavity was decreased in length by about $\lambda/20$ to bring about partial unlocking. The reading from the frequency counter was again recorded for times when the oscilloscope showed stable beat signal. The difference $\Delta\nu_1$ between these two readings represented the change in the beat signal as the laser became partially unlocked. (2) Secondly, the unit oscillator was reduced in frequency so that this time the beat note was slightly less than 30 MHz. Following the same measuring procedures as in (1), another frequency difference $\Delta\nu_2$ was obtained. In the event that there were missing counts while performing measurements on the unlocked laser, $\Delta\nu_1$ would be larger than $\Delta\nu_2$. Otherwise the two values should be equal. Table 1 shows results of a typical run. Experiments were repeated over a period of several days. The intermode beat frequency of the self-locked laser was found to be higher than that of the unlocked laser by approximately 600 Hz.

2) Error consideration

The biggest experimental error was due to the small change in laser power as the laser was tuned across the Doppler profile. It was observed that the average laser power changed by 0.02 db as the mode frequencies were varied over a range of 140 MHz. To estimate

the amount of error introduced, the intermode beat frequencies as a function of laser power were measured. The laser was first adjusted to give stable single-pulsing at a fixed position for the cavity modes. By varying the cavity loss with the aperture, relative beat frequencies corresponding to single pulsing at different laser power levels could be measured. Figure 6 shows the experimental result. From the slope of the curve, it is found that a change of 0.02 db in laser power results in a frequency change of 84 Hz.

Table 1

Intermode Beat Measurements for the Locked and Unlocked Laser

(1) Beat frequency = ~ 106 MHz + Mhz + F_1 (or F_1')

F_1 for the self-locked laser	F_1' for the unlocked laser	$\Delta\nu_1 = F_1 - F_1'$
30.7 KHz	30.1 KHz	0.6 KHz
30.7 KHz	30.0 KHz	0.7 KHz
30.8 KHz	30.1 KHz	0.7 KHz
30.7 KHz	30.2 KHz	0.5 KHz
		Ave. 0.61 KHz

$\Delta\nu_1 \simeq 610$ Hz.

(2) Beat frequency = ~ 106.2 MHz + 30 MHz - F_2 (or F_2')

F_2 for the self-locked laser	F_2' for the unlocked laser	$\Delta\nu_2 = F_2' - F_2$
191.2 KHz	191.7 KHz	0.5 KHz
191.2 KHz	191.8 KHz	0.6 KHz
191.1 KHz	191.9 KHz	0.8 KHz
191.2 KHz	191.8 KHz	0.6 KHz
		Ave. 0.61 KHz

$\Delta\nu_2 \simeq 610$ Hz.

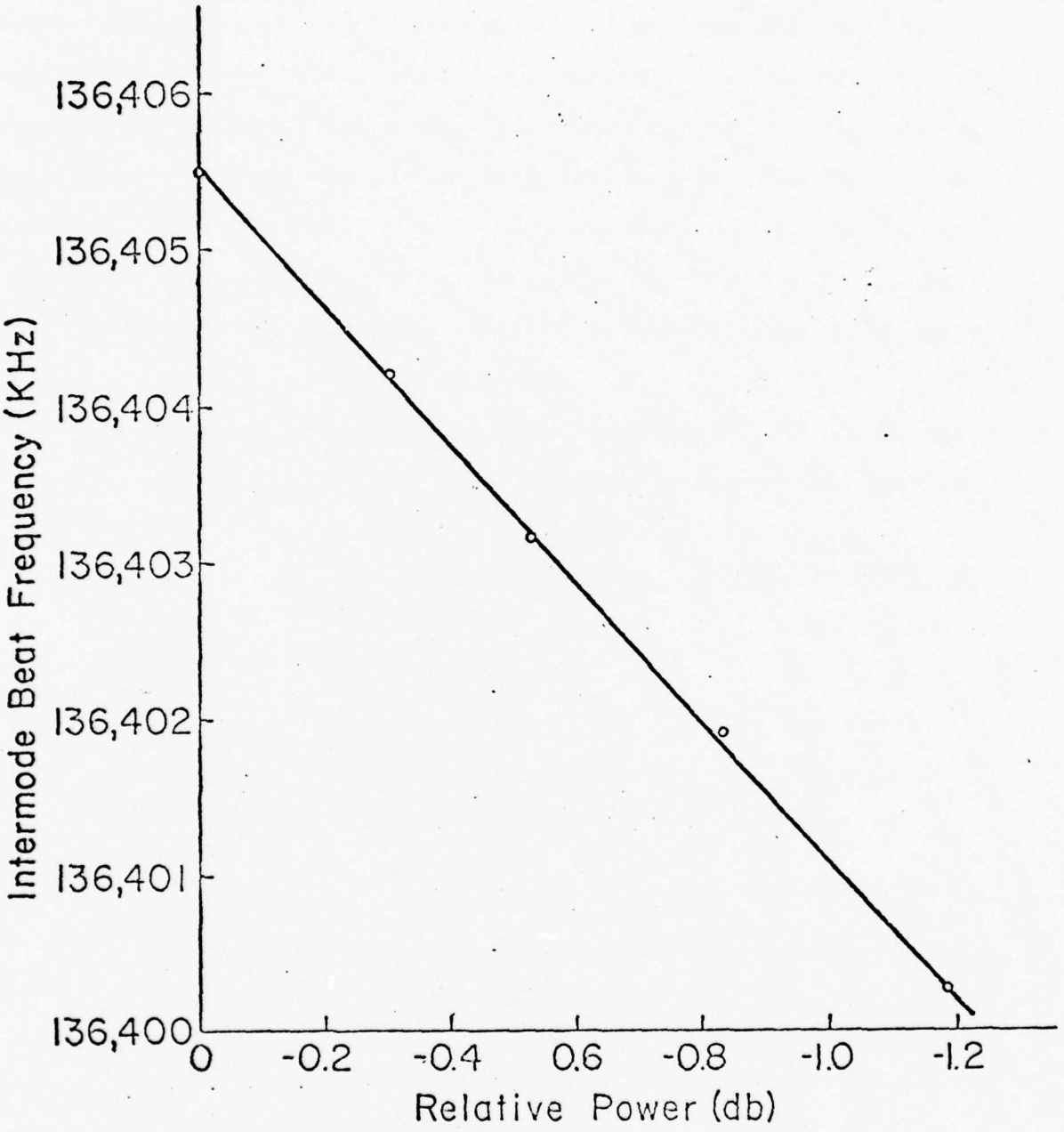


Figure 7. Intermode beat frequency vs. relative laser power. The zero decibel point corresponds to an internal one way power of 290 mW.

Other experimental errors resulted from the one count ambiguity of the frequency counter and the small change in cavity length by the PZT element attached to the mirror. The one count error is inherent to all counters due to the phasing between the timing pulse that operates the electronic gate and the pulses that pass through the gate to the counter. For the present experiment, the gate time was set at 0.1 second and the counting error thus introduced would be 10 Hz. Our experiment required that the cavity length be slightly changed so that the laser mode frequencies could be increased by about 15 to 20 MHz for the laser to switch from locked to unlocked. Accordingly, the spacing between adjacent modes would also be increased. Since the intermode spacing ν is given by $\nu = \frac{c}{2L}$, the change in the frequency spacing due to the cavity variation is

$$d\nu = -\nu \cdot \frac{dL}{L}$$

By substituting ν = 136 MHz, L = 110 cm and knowing that a change of the cavity length by $\lambda/2$ corresponds to shifting the mode frequencies by 136 MHz, $d\nu$ is found to be 5 Hz. Hence the maximum experimental error that could arise from the power change, the instrument counting error, and the change in cavity length is about $\pm$ 100 Hz.

From Eq. (10) with δ = (600 $\pm$ 100) Hz, $\Delta\omega \simeq$ 136 MHz and $v_g(\text{lock}) \simeq 3 \times 10^{10}$ cm/sec, the group velocity of the self-locked laser in the laser cavity is found to be faster than that of the unlocked laser by 4.4 parts in 10^6, or by (1.3 $\pm$ 0.2) $\times 10^5$ cm/sec. Since the gain medium has occupied about half the length of the

cavity, therefore, it is concluded that the group velocity of the self-locked pulse in the gain medium is larger than the group velocity of the unlocked laser by about 9 parts in 10^6 or $(2.6 \pm 0.4) \times 10^5$ cm/sec.

References

1. B. K. Garside, IEEE J. Quantum Electron. QE-5, 97 (1969).

2. B. K. Garside, IEEE J. Quantum Electron. QE-8, 471 (1970).

3. G. R. Willenbring, "Self-mode Locking in Inhomogeneous broadened CW Lasers", Ph.D. Thesis, University of Minnesota, 1973.

4. D. M. Thymian and J. A. Carruthers, IEEE J. Quantum Electron. QE-5, 83 (1969).

5. J. A. Carruthers and T. Bieber, J. Appl. Phys. 40, 426 (1969).

6. G. R. Willenbring and J. A. Carruthers, J. Appl. Phys. 41, 5040 (1970).

7. F. R. Faxvog, C. N. Y. Chow, T. Bieber and J. A. Carruthers, Appl. Phys. Lett. 17, 192 (1970).

8. F. R. Faxvog and J. A. Carruthers, J. Appl. Phys. 41, 2457 (1970).

C. Phase Relation between Modes in Self-Locked Lasers

1. Introduction

Self-mode locking, or self-pulsing, in a CW laser is a spontaneous condition in which the oscillating modes become equally spaced in frequency with fixed phase relationships.[1-5] The modes usually add together in such a way as to produce a large amplitude modulation of the electric field within the cavity so that one or more pulses of light is travelling back and forth in the cavity. The observation that the duration width of the pulses is often approximately the inverse of the width of the frequency spectrum has led at least one observer[1] to suggest that all of the modes are exactly, or very nearly, in phase at one time. The only reported measurement[6] gave indirect evidence that in a self-pulsing He-Ne laser the modes were very nearly in phase, although the experimental results could not be considered conclusive. The research reported here is concerned with new measurements of mode phases. Although self-locking of some transverse modes has been observed, this investigation was concerned only with lasers operating in the longitudinal modes. This work has been published in the Technical Report issued August 1973 and only a brief outline will be given below.

The basis for the experiment for measuring mode phases has been provided by a new analytical approach to self-locking in medium-power CW lasers. The results of the analysis indicate that there is no fundamental reason for the relative phase angles between modes to be identically zero. Therefore it was important to devise an experimental technique which could provide more detailed information on the relative phases of specific modes. The experimental results indeed showed that the modes are not all in

phase, and in particular one of the modes has a lagging phase angle of about 40°.

Self-locking was first reported by Crowell[1] in a He-Ne laser operating on the 632.8 nm transition. It has since been observed in He-Cd^+,[7,8] Ar^+,[9] and Kr^+ [10] lasers in the visible region of the spectrum and in He-Ne,[11] He-Xe,[11] CO_2,[12-14] and CO [15] lasers in the infrared. All of these are gas lasers for which the inhomogeneous Doppler-broadened linewidth is greater than, or approximately equal to, the homogeneous pressure-broadened linewidth. Hence they all have at least partially inhomogeneously-broadened gain profiles and are inherently multimode lasers. They are ordinarily operated continuously (CW) so that when they are self-locked the output is in the form of a continuous train of pulses of stable shape and constant repetition rate.

Self-locking is believed to occur because the oscillating modes are coupled through the nonlinearity of the saturated gain medium of the laser.[16] Mode locking can also occur when a saturable absorber is placed in the laser cavity,[17] and in that case the main coupling is through the nonlinearity of the absorbing material. Mode locking can also be induced by modulating the amplitude (AM)[18,19] or phase (FM)[20,21] of the radiation in the cavity at a frequency near the intermode beat frequency. For these cases the modes are coupled through a modulating element, often a small crystal in the cavity.

The longitudinal modes of a laser must satisfy the boundary conditions for resonant modes of the cavity. Even when part of the cavity is filled with active gain material, which is dispersive,

the resonant condition can be stated simply if given in terms of the wavelength. In the plane-wave approximation, the resonant condition can be stated simply if given in terms of the wavelength. In the plane-wave approximation, the resonant condition of $L \tilde{=} q\lambda_q/2$ where λ_q is the wave-length of the qth mode and 2L is the round-trip distance of the resonant cavity gives the mode frequencies as $\nu_q = q_c/2n(\nu_q)L$ where c is the free-space velocity of light and $n(\nu_q)$ is the index of refraction due to the dispersion of the gain medium. Those modes within the gain bandwidth of the inverted medium will oscillate.

In an unlocked laser the amplitudes and phases of the modes fluctuate randomly, and the frequency interval between modes is, in general, not constant because of the nonlinear variation of the refractive index with frequency.[4] However, when a laser is self-locked, the modes are precisely equally spaced in frequency, with constant phases and the mode amplitudes are very stable.[4,25] The result is a highly stable repetitive waveform with a repetition rate equal to the intermode frequency spacing. The exact shape of the waveform is determined by the relative phase angles between the modes. For the most common type of self-locking the relative phases are thought to be near zero. The laser output then consists of a train of narrow pulses separated by the round-trip transit time $T \tilde{=} 2L/c$. Other phase relationships, can result in two or more pulses in the cavity,[2,3,26] was primarily aimed at analyzing single pulsing.

In a self-locked laser the modes are exactly equally spaced in frequency whereas inspection of the dispersive characteristics of the gain medium would indicate that the modes should not be

equally spaced.[16,27,28] This implies that most of the modes of a self-locked laser are oscillating at frequencies slightly different from those of a completely unlocked laser.

The possibility of locking of modes to injection signals, or combination tones, arising from mode interactions in the saturated gain medium was first suggested by Lamb[16] in his general theory of an inhomogeneously-broadened gas laser. The theory involves the derivation of a set of self-consistent equations for determining the frequencies, amplitudes and phases of the oscillating modes. It was demonstrated that there existed steady-state solutions to those equations, for the case of three modes, in which there was equal frequency spacing and time-independent phase angles, but the actual values of the relative phase angles were not computed.

Other authors have further analyzed self-locking of three modes using Lamb's theory. Bambini[29] and Sargent[30] independently showed that for symmetrical tuning of the mode frequencies, with one mode exactly at the center of the line, the theory predicts that locking always occurs with relative phase angles of either 0° or 180°. The first case, in which all of the modes are in phase at one time, results in maximum amplitude variation and is called the AM case. For the other, the FM case, the modes on either side of the central mode have opposite phases resulting in a pure frequency modulated optical carrier. Sayers and Allen[31] have done extensive computer solutions of Lamb's three-mode equations for several cases of nonsymmetrical tuning. The results predict that locking occurs over a fairly narrow range of tuning around line center, and that the relative phase angles vary widely depending

on the tuning. Experimental observations of the locking range in a three-mode He-Ne laser[32] appear to agree with the theoretical predictions. These authors have not made calculations for more than three modes, presumably because of the complexity of the coupled nonlinear differential equations. However, Chen[33] has extended Lamb's calculations to more than three modes and computed the locking range for multimode He-Ne and $He-Cd^+$ lasers.

A limitation of the Lamb theory is the requirement that the holes burnt in the gain profile be narrow and nearly isolated. A condition not typical in self-locked He-Ne lasers. Measurements[34,35] indicate that the collision-broadened linewidth in a He-Ne laser having a total pressure of 2.5 Torr is about 400 MHz. This is a significant fraction of the Doppler-broadened width of about 1500 MHz and about three times as large as a typical intermode frequency spacing of 130 MHz. Furthermore, for large saturation the holes are wider than the homogeneous linewidth.[27] Thus there is an overlap between holes under highly saturated conditions resulting in a gain profile which is practically flat in the frequency range over which there are oscillating modes. Experimental evidence supporting this conclusion has been provided by Garside[28] who has found that dispersion calculations based on the assumption of a flat gain profile agree well with best frequency measurements in a He-Ne laser. It thus appears that the He-Ne laser is midway between the homogeneous and inhomogeneous extremes. This makes the theoretical description very difficult, and an approximate analysis may be required.

Another limitation of the Lamb theory, which is also encountered in the theory of a homogeneous laser, lies in the method of solving

the coupled nonlinear differential equations describing the behavior of the active medium in the presence of the radiation field. An iterative procedure is most often used which is valid only for near threshold conditions so that there is no appreciable gain saturation.[16] A typical multimode self-locked laser operates far above threshold and may be 50% saturated or more. However, for self-locked He-Ne and $He\text{-}Cd^+$ lasers the fluctuations in gain around the average saturated value are probably small. This conclusion is supported by pulse velocity measurements[8,36] which show that the pulse velocity is approximately equal to the group velocity associated with the average dispersion. If the gain fluctuations were large they would significantly affect the pulse velocity,[37] and this is not observed. Furthermore, the time constants for recovery of the inversion in the He-Ne [29] and $He\text{-}Cd^+$ [38] lasers are larger than the time between pulses so that in the steady state only small gain fluctuations can occur. For small gain variations an iterative procedure can be used under conditions of large saturation provided that the average saturated gain is known. The average saturation can ordinarily be estimated from knowledge of the small-signal gain and the output coupling of the laser mirrors.

2. Results

An experiment was designed and the apparatus constructed for directly measuring the relative phase angles between the spectral components of a linear self-locked He-Ne laser operating on the 632.8 nm transition with about 7 oscillating modes. The method used was to isolate a pair of adjacent modes using tunable confocal interferometers in a tunable Mach-Zehnder optical bridge and then

recombine them to form an amplitude modulated light beam at the intermode beat frequency $\Delta\nu$, generated by the mode-locked pulse train. By using a sliding retroreflector similar to that used by Fork and Pollack,[29] the phase of the modulation from the pulse train was adjusted to create a null in the total signal at $\Delta\nu$. A high-speed photo-multiplier was used as the optical detector followed by a heterodyne mixer and 30 MHz I.F. amplifier. By starting near the center of the spectrum and working in adjacent pairs out to the edges, the relative phase angles of all of the spectral components can be deduced.

The experimental data shows that for the laser used in the experiment the relative phase angles are indeed non-zero, and that one particular mode toward the high-frequency end of the spectrum lags the others in phase by about 40°. Thus it appears that self-pulsing does not necessarily mean maximum spiking as is sometimes assumed. The results are complicated by the highly asymmetric shape of the frequency spectrum of the laser used in the experiment. The exact cause of this asymmetry in a single-isotope laser is uncertain, but it is known to disappear in a unidirectional ring laser.[39] It is concluded that similar phase measurements should be made for a travelling-wave ring laser to allow a detailed check of the theory developed in this investigation.

The purpose of the investigation was to achieve a better understanding of self-pulsing in multimode laser oscillators. Although self-locking has received considerable attention since its discovery about ten years ago, the precise nature of the locking mechanism has remained in doubt. While it has long been recognized that third-order polarization sidebands generated by the nonlinearity of the

saturated gain medium may act as injection signals to lock the modes one to another, the precise nature of the locking process has not been completely analyzed for the wide range of conditions over which locking is observed.

The analytical method involves calculating the sidebands which are generated in a self-locked He-Ne laser by the saturated gain medium. The concepts have been developed for a purely homogeneous laser and were then applied to an inhomogeneous laser with uniform saturation by estimating the magnitude of the gain fluctuations and using the dispersion calculations of Garside. The assumption of small gain fluctuations allowed an approximate solution to the polarization equations. The assumption that the gain fluctuations are the same at the center of the line as at the edges is an over-simplification that probably results in significant error, particularly for the sidebands generated at the edges of the frequency spectrum. In addition, only the fluctuations at the fundamental best frequency, $\Delta\omega$, were considered while higher-order harmonics were neglected. However, the main purpose of the calculations was to outline a method of computing the sidebands and to examine their role as injection signals for locking the modes. For a more detailed application of the theory to a particular laser system, a new method for calculating the gain fluctuations for the inhomogeneous medium must be developed.

The calculations indicate that the third-order polarization sidebands have phase angles nearly 180° from the corresponding electric fields so that their main effect is to change the phase velocities of the modes, and this can be interpreted as a change in

the index of refraction. An analysis of locking of modes to the sidebands has revealed that, at locking threshold, injection locking is equivalent to changing the index of refraction so that it has the correct value for oscillation at the locked frequency. The amount of the index correction depends upon the relative phase angles, and there appears to be no fundamental reason for the relative phase angles in a self-locked laser to be identically zero.

The experimental results indeed show that the phases are not zero, and in a particular case one mode is lagging the others in phase by about 40°. The results for the other modes show phase angles different from zero, but probably by smaller angles. The results are complicated by the highly asymmetric nature of the frequency spectrum of the laser used in the experiment.

The cause of the asymmetry in a single-isotype laser appears to be related to mode competition since it disappears in a unidirectional He-Ne ring laser. For an asymmetric spectrum, the exact position of the center frequency of the transition is not know, making it difficult to estimate the values of the susceptibilities at the various mode frequencies. Therefore, it now appears that in order to make a detailed check of the theory, similar phase measurements should be made for a unidirectional travelling-wave ring laser.

References

1. M. H. Crowell, IEEE J. Quant. Electron, QE-1, 12 (1965).
2. T. Uchida and A. Ueki, IEEE J. Quant. Electron QE-3, 17 (1967).
3. F. R. Nash, IEEE J. Quant. Electron QE-3, 189 (1967).
4. F. R. Faxvog, M. S. Thesis, University of Minnesota (1968).
5. P. W. Smith, Proc. IEEE 58, 1342 (1970).
6. P. W. Smith, Optics Comm. 2, 292 (1970).
7. F. R. Faxvog, G. R. Willenbring, and J. A. Carruthers, Appl. Phys. Letters 16, 8 (1970).
8. G. R. Willenbring and J. A. Carruthers, J. Appl. Phys. 41, 5040 (1970).
9. O. L. Gaddy and E. M. Schaefer, Appl. Phys. Letters 9, 281 (1966).
10. S. J. Heising, S. M. Jarrett, and D. J. Kuizenga, J. Quant. Electron QE-7, 205 (1971).
11. H. H. Kim and H. Marantz, J. Quant. Electron QE-6, 749 (1970).
12. H. Ito and H. Inaba, Optics Comm. 1, 61 (1969).
13. T. J. Bridges and P. K. Cheo, Appl. Phys. Letters 14, 262 (1969).
14. S. Marcus and J. H. McCoy, Appl. Phys. Letters 16, 11 (1970).
15. Ph. Brechignac and F. Legay, Appl. Phys. Letters 18, 424 (1971).
16. W. E. Lamb, Jr., Phys. Rev. 134, A1429 (1964).
17. A. G. Fox, S. E. Schwarz, and P. W. Smith, Appl. Phys. Letters 12, 371 (1968).

18. L. E. Hargrove, R. L. Fork, and M. A. Pollack, Appl. Phys. Leters 5, 4 (1964).

19. M. DiDomenico, Jr., J. Appl. Phys. 35, 2870 (1964).

20. S. E. Harris and O. P. McDuff, IEEE J. Quant. Electron, QE-1, 245 (1965).

21. E. O. Ammann, B. J. McMurtry, and M. K. Oshman, IEEE J. Quant. Electron, QE-1, 263 (1965).

22. A. G. Fox and T. Li, Bell System Tech. Journal 40 453 (1961).

23. K. Kohiyama, T. Fukioka, and M. Kobayashi, Proc. IEEE 56, 333 (1968).

24. Y. Watanabe, T. Fujioka, and M. Kobayashi, IEEE J. Quant. Electron, QE-4, 880 (1968).

25. S. A. Schmitt, M. S. Thesis, University of Minnesota (1968).

26. R. E. McClure, Appl. Phys. Letters 7, 148 (1965).

27. W. R. Bennett, Jr., Phys. Rev. 126, 580 (1962).

28. B. K. Garside, IEEE J. Quant. Electron, QE-5, 97 (1969).

29. A. Bambini and P. Burlamacchi, IEEE J. Quant. Electron QE-4, 101 (1968).

30. M. Sargent III, IEEE J. Quant. Electron QE-4 343 (1968).

31. M. D. Sayers and L. Allen, Phys. Rev. A 1, 1730 (1970).

32. D. G. C. Jones, M. D. Sayers, and L. Allen, J. Phys. A (Gen. Phys.) 2, 95 (1969).

33. T. S. Chen, Ph.D. Thesis, University of Minnesota (1971).

34. P. W. Smith, J. Appl. Phys. 37, 2089 (1966).

35. C. V. Shank and S. E. Schwarz, Appl. Phys. Letters 13, 113 (1968).

36. F. R. Faxvog, C. N. Y. Chow, T. Bieber, and J. A. Carruthers, Appl. Phys. Letters 17, 192 (1970).

37. P. W. Smith, IEEE J. Quant. Electron QE-6, 416 (1970).

38. M. D. Klein and D. Maydan, Appl. Phys. Letters 16, 509 (1970).

39. B. K. Garside, IEEE J. Quant. Electron. QE-4, 940 (1968).

D. Theory of Ultrashort Pulse Generation

The problem of ultrashort pulse generation in lasers was investigated. Measurements based on the intensity correlation technique indicate the presence of spontaneous, pico-second pulses in most solid-state lasers as well as oscilloscope pictures of the intensity variation at the output of gas lasers which show the presence of pulses of approximately a nanosecond duration. Most measurements up to the time the theoretical work was carried out had been performed on Fabry-Perot-type lasers whereas the theoretical investigations of the pulse phenomena had been confined to infinitely long laser media or ring lasers supporting pulses in one direction only.

An analysis of ultrashort pulses in Fabry-Perot lasers and ring lasers based on two opposing waves was carried out. The method which is used was an extension of even earlier work on self-pulsing in ring lasers. The extension was non-trivial because the strong nonlinearities intrinsic to the laser material in highly-pumped lasers prevents the application of the superposition principle. Significant differences between the two cases were found.

The basic equations were derived according to a semi-classical radiation theory. In this derivation the system was restricted to a homogeneously broadened two-level system with phenomenological damping and pumping of the system. The field was decomposed into oppositely-traveling waves and equations of motion for the slowly varying amplitude variables were obtained. The oscillatory space dependence of the inversion arising from the interference of the oppositely-traveling waves was included. This inversion was shown to contribute to the nonlinear coupling between the waves.

The nonlinear partial differential equations of the laser were investigated for the boundary conditions of the oppositely-traveling waves present in a ring laser. The stability of the system was investigated. The laser equations were solved numerically in the unstable regions. For real-field variables the characteristic ultrashort pulses were shown to develop and propagate.

The complexity of the set of normal mode equations resulting from the analysis makes them less suitable for numerical analysis than expected. Therefore, equations were solved numerically with the Fabry-Perot boundary conditions. A proper set of parameters was obtained from the stability investigation of the mode equations. Due to the end reflections of a laser, all the energy of the forward wave is transferred to the backward wave at the mirrors. The result of this allows one to obtain, in the homogeneously-broadened Fabry-Perot laser, quasi-stationary solutions in the form of oppositely-traveling waves in contrast to the opposing-wave ring laser. The solutions of the real-field laser equations apparently failed to be strictly periodic. They are, therefore, different from the solutions of a one-way ring laser. A slow modulation of the pulses was observed for various choices of parameters and characterizes the pulse solutions of a Fabry-Perot laser.

E. Analysis of Mode Locking

A theoretical model was developed to describe the observations of self-locking in multi-mode gas lasers. The model is based upon an extension of the semi-classical theory of lasers given by Lamb and includes the effects of collisional-line broadening in the semi-classical expression for the polarization. A consequence was that the nonlinear terms produced self-locking over a range of values the ratio of loss to unsaturated gain.

Self-mode locking had been discussed earlier theoretically and experimental observations have also been reported. This work derived the theory of self-mode locking based on combinational tones as discussed by Lamb where the combination frequencies correspond to the oscillation frequency of one of the modes producing the nonlinear polarization. The nonlinear polarization terms may be considered acting as a source for injection onto which the three modes phase-lock. In this earlier work, collision effect, on the line width, had been neglected.

The intent of the present work was to provide an extension of Lamb's model to more than three modes. The criteria for self-mode locking was found to be expressed as a polynomial expression for the ratio of loss to unsaturated gain. In this method, an inequality was found to define the region over which the ratio satisfies the condition of self-mode locking. When the ratio exceeds a certain critical value, all the modes above threshold are self-locked and the laser output consists of periodic pulses. The theoretical analysis was supported by experiments on self-mode locking of

longitudinal modes in He-Ne and He-Cd lasers with satisfactory agreement between predicted and observed modes being self-mode locked.

F. Gain Studies in CO_2 Lasers

The primary mechanism responsible for limiting the gain in CO_2 discharges has been shown to be related to the gas temperature. In discharges of conventional CO_2 lasers, calculations of the radial gas temperature profile as a function of discharge current were carried out and related to small signal gains measured in CO_2 discharges. A series of measurements of the small signal gain as a function of radial position and discharge current were conducted. At high currents, and correspondingly high temperatures, the radial profile of the gain is lower at the center of the tube than near the tube wall. However, at low currents and correspondingly low temperatures, the radial gain profile follows the J_o Bessel function distribution of the electron density as predicted by the theory of the positive column. A theory was developed accounting for radial gain profiles as a function of the total discharge current.

A method, offering an improvement in gas cooling over conventional CO_2 lasers was demonstrated, by increasing the axial flow velocity of the gas, calculations show the discharge temperatures can be substantially reduced by the removal of the hot gas and molecules still in excited states. A technique was described employing a number of consecutive small discharges which successfully increased the power generation per unit volume. The technique can be scaled; consequently the possible power from the laser is limited mainly by the size of gas supply and pump.

This work has been published in the literature and in technical reports by Franzen.

G. CO_2 Laser Plasma Studies

The neutral and ionic population of a plasma in a CO_2 laser gas mixture was analyzed mass spectrometrically. Comparative measurements of the CO_2 concentration at the cathode and anode side of the discharge showed that the strongest regeneration of CO_2 is at the cathode side.

The oxidation mechanisms of CO (regeneration of CO_2) in the $He-N_2-CO_2$ plasma were consistent with:

$$O(D) + CO \rightarrow CO_2$$

or alternatively

$$O(D) + CO_2 \rightarrow CO_3$$

$$CO_3 + CO \rightarrow 2CO_2 \ .$$

When water vapor is added to the triple mixture, the CO_2 is more effectively regenerated and the reaction $OH + CO \rightarrow CO_2 + H$ plays probably an important role.

The molecule CO_3 was observed here for the first time based on the mass spectra of the gas mixtures with water vapor, where a mass 60 is observed.

In a sealed-off CO_2 laser deposits are formed from the gas mixture. The removal of the gas in this way limits the lifetime of the laser. Fragments of these deposits were analyzed mass spectrometrically and their possible composition found. Several characteristics of the deposit are: the property to regenerate CO_2 and the property to emit positive ions of mass 39 and 41 under hot conditions, when the discharge is turned off.

H. Mass Spectroscopic Studies of CO_2 TEA Laser Discharge

1. Introduction

In work previously carried out in the Department of Electrical Engineering, a transversely-excited, high-pressure CO_2 laser (TEA laser) was constructed and its operation studied. This type of laser has a pulsed electrical discharge transverse to the optical axis and uses a CO_2:N_2:He gas mixture at pressures of several hundred mmHg.

The laser constructed here was found to reach a maximum output power at pressures of 100 to 200 mmHg at pulse repetition rates of 5 pps with flowing gas mixtures. The power decreased at higher pressures, and some of this decrease was shown to be due to gas heating effects. It was thought that gas decomposition effects could also be playing a part, with discharge products harmful to laser action diffusing away more slowly at the higher pressures.

Since mass spectroscopic studies had been made in this laboratory on the CW longitudinal discharge CO_2 and CO lasers[2-6], a similar study of the CO_2 TEA laser discharge was made. It was expected that decomposition of CO_2 into CO and O_2 would take place in the TEA laser as it does in the longitudinal discharge laser[2,5], but the amount of decomposition and the time to reach an equilibrium composition were to be investigated for the new type of discharge. A search was made for other discharge products such as NO, and NO_2 not found in significant quantities in the longitudinal discharge CO_2 laser, but perhaps formed in the high-current pulsed TEA laser discharge.

2. Apparatus

The original TEA laser was constructed of a 200 cm length of 5 cm diameter plexiglass and had a very high ratio of total internal

volume to active discharge volume. For the experiments reported here, a discharge tube was built with a similar electrode configuration to the TEA laser but with a much lower ratio of internal volume to discharge volume. This requires much shorter times to reach equilibrium in the gas composition with the discharge on.

The discharge tube used was constructed of plexiglass and had internal dimensions of 1.2 cm wide, 5 cm high, and 43 cm long. A pin electrode was formed by 58 individual 1 KΩ resistors (1 watt, 5%) with their leads epoxied into holes drilled on 6 mm centers along the top of the discharge tube. The lower electrode was a 1.27 cm brass rod spaced 2.54 cm from the pin electrodes. A capacitor of .0043 μF was charged to a maximum of 20 KV and discharged through the tube by a triggered spark gap at a rate variable up to 20 pps.

Gas samples could be taken from the tube by either of two 41 cm^3 sample tubes, closed by stopcocks and fastened to the discharge tube by vacuum disconnects. Samples of gas so collected could then be analyzed by the RF quadrupole mass spectrometer used in previous experiments[3,6].

3. Experiment

A premixed gas consisting of a CO_2:N_2:He in the ratio 1:1:2 was admitted into the evacuated discharge tube to a pressure of 200 mmHg, and tube closed off. The sample tubes both had been open to the discharge tube, and one was now closed to retain a sample of the gas before discharge. The pulsed discharge was run at 15 pps with the energy storage capacitor being charged to 16 KV. After the discharge was turned off, the gas composition was allowed to reach equilibrium throughout the tube, and the second sample tube

was closed. Both sample tubes were taken to the mass spectrometer and analyzed to determine changes in composition caused by this discharge.

4. Results

It was found that a significant amount of CO_2 decomposition occurred in the TEA laser discharge. The CO_2 mass peak (M=44) decreased from the "before" to the "after" sample, while the M=28 peak (CO and N_2) and M=32 (O_2) peak increased. The decrease in the CO_2 peak height with discharge running time is shown in Figure 1. The gas mixture was CO_2:N_2:He in the ratio 1:1:2 at a pressure of 200 mmHg, and the pulse rate was 15 pps. The curve drawn corresponds to 19% decomposition of CO_2 exponentially with a time constant of 53 min. This time constant is for our discharge tube and experimental conditions only, and is determined by the CO_2 decomposition rate, the pulse repetition rate, the discharge tube geometry, the gas mixture used, and the discharge parameters. The steady-state CO_2 decomposition of 19% is comparable to that found for the CW longitudinal-discharge CO_2 laser[5].

No measurable increases in mass numbers associated with other molecular species such as NO, NO_2 were found to occur during the discharge. The chemistry in the CO_2 TEA laser discharge thus seems similar to that in the longitudinal-discharge, low-pressure CO_2 laser. These observations are consistent with the fact that the ratio of electric field strength to pressure (E/P ratio) is similar for both lasers, of the order of 10^4 volts/cm-atmosphere.

Nonuniformities in the discharge and the formation of bright arcs with this electrode configuration limited operation to about

250 mmHg pressure. Problems with the mass spectrometer prevented obtaining good data for gas mixtures richer in He. Any future investigations of this type should study mixtures of about 80% He at pressures near atmospheric which typify present-day CO_2 TEA lasers.

References

1. William G. Patrek, Plan B Paper for M.S. Degree, University of Minnesota, 1971.
2. Third Annual Report of Research on Project Grant ONR #N00014-68-A-0141-0002, September 1970, University of Minnesota, P. 11.
3. Fourth Annual Report of Research on Project Grant ONR #N00014-68-A-0141-0002, September 1971, University of Minnesota, P. 36.
4. J. Freudenthal, IEEE Journal of Quantum Electronics QE-6, 507 (1970).
5. J. Freudenthal, Journal of Applied Physics 41, 2447 (1970).
6. G. B. Hocker, IEEE Journal of Quantum Electronics QE-7, 535 (1971).

I. Noise in Optical Heterodyne Detection

1. Introduction

The theory of optical heterodyne detection predicts that the limiting noise in the optical detector is due to pump processes and the amplified noise of the incoming radiation. The purpose of this study was to establish the second effect by direct experiment at 10.6 microns using paraelectric detector.

The theory of optical heterodyne detection gives the following important results;

1) the spectral intensity,

$$S_1(f) = 2q\ (1 + 2\eta)\ I_p \qquad (1.1)$$

for photodiode in terms of current, where q is the electron charge, η is a quantum efficiency of the photodiode and I_p is the pump signal current. The term $2qI_p$ is due to the pump signal, and the term $4qI_p\eta$ is due to the incoming radiation. Within certain limits, it is independent of the intensity of incoming radiation.

Also $S_i(f)$ can be expressed in terms of the average pump signal power $\bar{P}_p$,

$$S_i(f) = (\alpha + 2\eta)\cdot 2c^2 h\nu\eta\ \bar{P}_p \qquad (1.2)$$

where $o = \frac{e}{h\nu}$, $\alpha = 2$ for photovoltaic cell and photoconductive detector, and $\alpha = 1$ for photodiode. The equation (1.2) is valid for proelectric detector if the radiation noise would be predominant over others, with $\alpha = 1$ and η is the effective quantum utilization factor. The term $\alpha\cdot 2c^2 h\nu\eta\ \bar{P}_p$ is due to the pump signal and the term $2\eta\ 2c^2 h\nu\eta\bar{P}_p$ is due to the amplified noise of the incoming radiation.

2) The signal-to-noise power ratio $\frac{S}{N}$ for heterodyne detection is,

$$\frac{S}{N} = \frac{2}{1 + 2\eta} \frac{I_1}{2eB} \tag{1.3}$$

for the photodiode. It is expressed in terms of incoming signal current I_1. The second term $\frac{I_1}{2eB}$ is the $\frac{S}{N}$ ratio for direct detection.

It can also be expressed in terms of the incoming radiation power $\bar{P}_1$ as,

$$\frac{S}{N} = \frac{2}{\alpha + 2\eta} \frac{\bar{P}_1}{2h\nu B} \tag{1.4}$$

where $\alpha = 1$ for photodiode and $\alpha = 2$ for photovoltaic cell and photoconductive detector.

For $\frac{S}{N} = 1$, the minimum detectable power of $\bar{P}_1$, $(\bar{P}_1)_{min}$ can be written as,

$$(\bar{P}_1)_{min} = h\nu \frac{\alpha + 2\eta}{\eta} \text{ watts/Hz} \tag{1.5}$$

at the bandwidth B=1. For pyroelectric detector,

$$\text{NEP} = \frac{\Sigma\, S_1(f)_H}{2\,\gamma^2 \bar{P}_p} \text{ watts/Hz} \tag{1.6}$$

where γ is the current responsivity at the beat frequency.

It is advantageous to make use of spatially coherent monochromatic laser light in superheterodyne detector experiments. Two CO_2 lasers of 10.6 microns in single mode operations were used as an input signal light and a local oscillator (pump signal). The beat frequency was stabilized by means of an electromechanical

control system and the measurements were made at 1.5 MHz since below about 100 KHz, the local oscillator laser light and the optical detector itself produce excess noise. However, above this frequency there is full shot noise.

2. Results

The experimental work carried out consisted of three parts:

a) direct verification of equation (1.2), and

b) direct verification of equation (1.5), with the photoconductive detector. A reasonable agreement with theory was shown

c) The measurement of NEP with an SBN pyroelectric detector gives the potential utility of this detector in heterodyne detection.

It was shown that there are two inherent noise sources in heterodyne mixing;

1) noise in the pump process,

2) amplified noise due to fluctuations in the arrival rate of signal quanta.

These two facts give the spectral intensity in heterodyne mixing as,

$$S_1(f) = \left(\frac{\alpha + 2\eta}{\alpha}\right) S(f)_{\text{pump}} \qquad (4.1)$$

$$= (\alpha + 2\eta) \cdot 2c^2 h\nu\eta \, \bar{P}_p$$

where η; quantum efficiency for photodiode, photovoltaic cell and photoconductive detector or the effective quantum utilization factor for pyroelectric detector if radiation noise is predominant over all other noise sources. Moreover,

$\alpha = 2$; for the photovoltaic cell and the photoconductive detector,

α = 1; for the photodiode and the pyroelectric detector. So far, the theory of heterodyne detection failed to take into account the second effect.

According to equation (4.1), $S_i(f)$ is independent of $\bar{P}_i$ and dependent on $\bar{P}_p$. The experimental verification of these facts was carried out.

a) The signal-to-noise power ratio for heterodyne detection is,

$$\frac{S}{N} = \frac{(\overline{I^2})}{S_i(f)} = \frac{2}{\alpha + 2\eta} \frac{\overline{\eta P_i}}{2h\nu B} \tag{4.2}$$

where α = 1; for the photodiode and the pyroelectric detector if radiation noise predominates,

α = 2 for the photovoltaic cell and the photoconductive detector, and

$\overline{I^2} = 2\gamma^2 \bar{P}_p \bar{P}_i$ at the beat frequency,

The minimum detectable input power $(\bar{P}_i)_{min}$ per unit bandwidth can be obtained for $\frac{S}{N}$ = 1 at B = 1 as

$$(\overline{P_i})_{min} = \frac{\alpha + 2}{\eta} \cdot h\nu \text{ watts/Hz} \tag{4.3}$$

However, for the pyroelectric detector the non-radiation noise sources predominate and in that case we define NEP as shown in equation (2.69)

$$NEP = \frac{\sum S_i(f) \; H}{22 \; \gamma^2 \; \overline{P_p}} \tag{4.4}$$

To obtain $(\overline{P_i})_{min}$ for the photoconductive detector, the $\frac{S}{N}$ ratio was measured as a function of $\overline{P_i}$. Using a measured value of $\eta = 0.143$ the value of $\frac{S}{N}$ ratio was manipulated to obtain $(\overline{P_i})_{min} = 3.68 \times 10^{-19}$ watts/Hz in comparison with the theoretical value of 8.0×10^{-19} watts/Hz. In the view of the long extrapolations this is a very good agreement. The measured values of $\eta = 14.3\%$ and $(\overline{P_i})_{min} = 3.68 \times 10^{-19}$ watts/Hz , are therefore quite compatible. ($B_{\overline{eff}}$ 2KHz)

b) For the pyroelectric detector, the voltage responsivity was measured and an experimental value of $\gamma = 0.133$ V/watt at 1.5 MHz was found. With an input circuit resistance R = 10K Ohms in parallel with input tuned circuit, the measured equivalent noise current was 5.0μA which is the same value of I_{eq} as expected for a resistance value of 10K Ohms. This means that the input circuit resistance noise predominates over all the other noise

$$NEP = \frac{2eI_{eq}}{(\frac{\gamma}{R})^2 \overline{Pp}} = 1.9 \times 10^{-14} \text{ watts/Hz}$$

at $\overline{P_p} = \frac{1}{4}$ watts. This is a factor of 10^2 better than Abrams and Glass[1] discussed for an amplifier noise limited case. It can be improved by using a larger value of R. Our measurement system was not stable enough, however, to increase R by an order of magnitude.

The key equation of heterodyne detection is the signal-to-noise power ratio, $\frac{S}{N}$. The conventional definition of $\frac{S}{N}$ ratio failed to recognize the presence of the amplified noise of the incoming radiation. The theory developed here fully considered this fact to evaluate the important formula of $\frac{S}{N}$ ratio for heterodyne detection. A reasonable experimental verification was obtained at 10.6 microns

for the photoconductive detector. A similar verification was found for a photodiode at 6328 Å[2]. However no reliable experiments were carried out with a photovoltaic detector operating at 10.6 microns.

There are some difficulties to accurately verify the theory experimentally if the value of η is too small, because factor $\frac{(\alpha + 2\eta)}{\alpha}$ is equation (4.1) would be close to unity, especially for an infrared detection.

The value of the NEP of the pyroelectric detector shows the advantages and potential usefullness for infrared heterodyne detection, in particular at room temperature operation. For improvement in the detector performance a device with a large coefficient is needed. This means a large pyroelectric coefficient and a small heat capacity per unit volume. The largest pyroelectric coefficient is at near the Curie temperature, but the operating point cannot be chosen too closely to that temperature because the operation of the device would become unstable. It is clear, however, that the pyroelectric detector that has the lowest NEP at 10 Hz is not necessarily the best heterodyne detector at 1.5M Hz.

J. The Raman Spectra of Proustite

1. Introduction

A study to determine and interpret the Raman spectrum of single crystal proustite was carried out. The Raman spectrum was observed using 6328 Å laser light for excitation, and a double grating spectrometer with photoelectric detection. The interpretation was based on group theory predictions along with predictions associated with simultaneously Raman and infrared active vibrational modes. Using group theory it was shown that proustite has 19 Raman active vibrational modes or phonons. Of these, 17 were observed in the Raman spectrum.

The number of first order Raman active modes was predicted by a group theory analysis of the crystal structure. The proustite crystal structure is characterized by a 14 atom unit cell having C_{3v} point group symmetry and R_{3C} space group symmetry. An analysis of these characteristics in conjunction with the symmetry properties of the point group was used to determine the symmetry of first and second order vibrations in the proustite unit cell.

It was shown that the symmetry of the polarizability tensor governing Raman scattering could be used to predict the number of Raman active modes of a particular symmetry along with the scattering geometries for observing them. The symmetry properties of the polarizability tensor elements were compared to the symmetry properties of the point group C_{3v}. This comparison made possible scattering geometry predictions under which phonons of specific symmetry corresponding to a particular tensor element could be observed. Orientations for observing TO transverse optic phonons, LO (longitudinal optic) phonons and phonons of mixed LO, TO character

with wavevectors having various orientations with respect to the crystal Z axis were determined.

In proustite all vibrational modes which are Raman active are also infrared active and the effects with modes which are simultaneously Raman are infrared active were investigated by considering a crystal lattice with only one such mode. Calculations showed that the splitting in frequency between the LO and TO phonons depended on the square root of the ratio of the static to the optical dielectric constants. There calculations provided a foundation for a second analysis which considered a crystal lattice with two modes which were simultaneously Raman and infrared active. Calculations illustrated the possibility of having a mixing between $A_1(Z)$ and E symmetry species modes under certain scattering geometries in violation of the group theory predictions. The degree of mixing was shown to be dependent on the relative strengths of the local crystal anisotropy which leads to group theory predictions and the electric field responsible for the LO, TO phonon frequency splitting. This mixing was shown to be responsible for a variation in the observed extraordinary phonon frequency with respect to the phonon propagation angle measured from the crystal C axis. The above analysis completed the background work necessary to systematically observe and interpret the Raman spectrum of single crystal proustite.

2. Results

The Raman spectrum of proustite was measured using Helium-Neon laser excitation at 6328 Å, a double grating spectrometer for dispersion and photoelectric detection. A variety of scattering geometries were used which involved changing incident and scattered light propagation and polarization directions. The purpose

in using these geometries was to obtain the information necessary to assign the observed phonons to predicted symmetries of a specific TO, LO, or mixed LO, TO nature. Both the frequency shift and peak intensity were recorded for each phonon.

The observed spectra were interpreted using the previously described theory to assign the phonons to specific species. Of the 6A and 13E symmetry modes predicted, 6A and 11E were observed. Also 7 second order modes were observed and assigned to symmetry species.

The fact that in proustite all vibrational modes are simultaneously Raman and infrared active means that a knowledge of its Raman spectrum provides information concerning its infrared properties. Infrared absorption measurements, which are generally more difficult to make than Raman measurements, are incomplete owing to a strong absorption in proustite beyond 14μm. This absorption region corresponds to the 715 cm^{-1} to 0 cm^{-1} Raman region. Observed first order Raman spectra are summarized in Table 4.

TABLE 4

$A_1(Z)$		E(-X) or E(Y)	
TO	LOO	TO	LO
31	43	21	21
136	136	49	490
184	184	63	63
281	289	104	104
362	367	120	120
734	732	222	222
		264	274
		331	354
		670	670
		700	700
		915	NOT OBSERVED

Table 4. The assignment of first order phonons whose shifts are given in cm^{-1}.

In this table the TO and LO phonon wavenumbers are given for phonons of specific symmetry.

In general it can be seen from this table that the LO-TO wavenumber splitting is small. For E symmetry phonons only those at 264 cm^{-1} and 331 cm^{-1} and for $A_1(Z)$ symmetry phonons only those at 31, 281, and 362 cm^{-1} exhibit any observable LO-TO wavenumber splitting. The largest percentage splitting was observed for the $A_1(Z)$ symmetry phonon at 31 cm^{-1}. Using the LO and TO wavenumber for this phonon the wavenumber splitting was calculated for a single phonon system. These calculations agreed with the predictions of equation (42).

For those phonons exhibiting an LO-TO wavenumber splitting all except the E symmetry 331 cm^{-1} phonon showed a behavior predicted for a material in which crystal anisotropy dominates the electric field. The 331 cm^{-1} showed a behavior predicted for a material in which the electric field dominates.

A comparison of the total number of phonons of a given symmetry species in Table 4 with those predicted by group theory shows that all $A_1(Z)$ symmetry phonons were observed while 11 of 13E symmetry phonons were observed.

Seven second order Raman modes were observed. Their wavenumbers, symmetry assignments and the wavenumbers of the phonons producing the second order effects are all summarized in Table 5.

TABLE 5

Wavenumber (cm^{-1})	Assignment	Participating Phonons (cm^{-1})
50	$A_1(Z) \times A_1(Z)$	184 - 136
432	E x E	221 + 221
474	$A_1(Z) \times E$	136 + 331
490	$A_1(Z) \times A_1(Z)$	136 + 362
542	E x E	222 + 331
608	$A_1(Z) \times E$	281 + 331
646	$A_1(Z) \times A_1(Z)$	281 + 362

Table 5. The assignment of second order phonons.

A comparison of the observed Raman spectrum to the infrared absorption spectrum of proustite, shown in Fig. 1, reveals that Raman phonons were observed corresponding to the only two infrared absorption peaks shown in the figure. The 731 cm^{-1} $A_1(Z)$ symmetry phonon corresponds to the 13.8μ (725 cm^{-1}) absorption and the 915 cm^{-1} E symmetry phonon corresponds to the 10.2 (980 cm^{-1}) absorption.

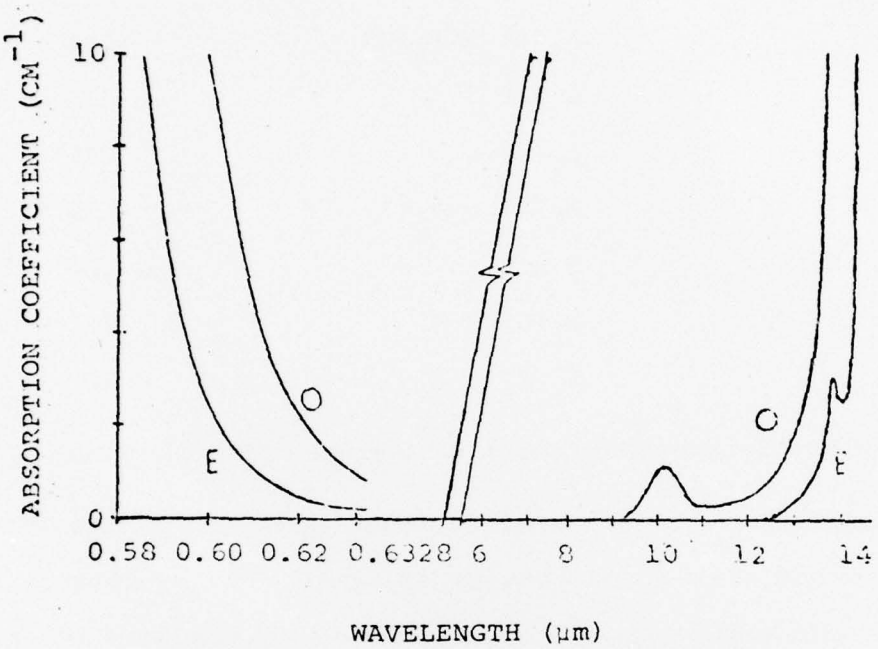


Fig. 1 The absorption spectrum of proustite according to Hulme et al.[1]. The propagation vector $\vec{k}$ of the incident radiation is along the crystal x axis. The curve labeled E is for the extraordinary ray in which the polarization direction is along the Z axis and curve labaeled O is for the ordinary ray in which the polarization direction is along the Y axis. The absorption coefficient α is defined by $I = I_o \exp(-\alpha x)$ where I and I_o are the transmitted and incident radiation intensities and x is the thickness of the crystal along the direction of radiation propagation.

K. The Nonlinear Susceptibility and Dispersion of Proustite

The study of the dispersion of the nonlinear susceptibility in Proustite is summarized below.

Measurements of the ordinary polarization absorption coefficient indicate separate vibrational modes at 915 and 1001 cm^{-1}. Insufficient data was available to assign the latter to either a fundamental or combination lattice mode. A comparison of the Raman spectra[2] with the results of Hobden[1] indicate that the primary vibrational contribution to the index of refraction is from vibration modes at 331 and 362 cm^{-1} for the ordinary and extraordinary polarizations, respectively.

Measurements of the coefficient for second harmonic generator from 930 to 1060 cm^{-1} have been made. No contribution to the nonlinear susceptibility from the 1000 cm^{-1} absorption was found although weak dispersion probably due to the primary lattice mode at 331 cm^{-1}, was observed. Since the 1000 cm^{-1} lattice mode was not observed, dispersion of the nonlinear coefficient in parametric fluorescence measurements by Hordvik, et. al.[9] must be attributed to dispersion of the electronic contribution.

The absolute magnitude of the effective nonlinear coefficients for phase-matched second harmonic generation at 946 cm^{-1} (10.58 micrometers) are 40×10^{-9} and 24.6×10^{-9} esu units for the additive and subtractive gemometries, respectively. The crystallographic coefficients are $|d_{22}| = 36 \times 10^{-9}$ esu and $|d_{31}| = 18 \times 10^{-9}$ esu.

References

1. M. V. Hobden, Opto-Electronics 1, 159 (1969).

2. J. S. Rayside, Ph.D. Dissertation (University of Minnesota, Minneapolis, 1973).

L. Optically Induced Gratings

1. Introduction

The interaction of two optical beams in adsorbing media has been observed to self-scatter as much as 10% of the incident ruby light and to scatter up to 30% of an additional probe beam. The scattered light was collimated and emerged from the sample at discrete angles. In these experiments, the incident waves were obtained from a ruby laser and allowed to interact in absorbing media (e.g. cupric sulfate or cryptocyanine dissolved in methyl alcohol or crystalline ZnO). A theory to describe these effects was developed based on diffraction from a periodic modulation of the index of refraction.

In the model describing the experiments changes in the couples index of refraction are assumed to be produced by the deposition of energy in the media by the incident beams. The spatial periodicity of the perturbation in the index of refraction results from the interference between the two coherent light beams. The net effect is the generation of either a phase or an amplitude diffraction grating. Experiments were shown to compare well with theoretical results based on this model. A simple periodicity in the complex index of refraction can be produced by energy adsorbed in an interference pattern producing local heating. Effects of this type when the interference pattern is produced by a pulsed beam can be studied by the time dependence of the optical scattering from the periodic structure.

Although the optical properties of a medium are independent of intensity at low light levels, with the intense optical fields

available from lasers, changes in the optical properties of a material can be induced by the applied optical field. In these cases the response to the applied optical fields becomes dependent on the instantaneous or the average intensity of the wave, and nonlinear response to the indigent light is observed.

In spite of the extensive use of the extrinsic type nonlinearity to produce changes in transmission or reflection (e.g. bleachable dye Q-switches), only a few experiments have used the incident light intensity to produce a spatially modulated change in the optical either through the linear or nonlinear phase changes. An interference pattern is an example of an intensity profile that could cause a spatial modulator of the optical properties within a medium. For two equally intense beams, the spatial variation of the intensity in the interference pattern is shown in Fig. 1. Mechanisms for the generation of the diffraction gratings and in absorbing media were studied.

Although different physical processes can be responsible for the production of the optically induced diffraction gratings, the resulting gratings can be classified as either amplitude or phase diffraction gratings. An amplitude grating is caused by a spatial modulation in the absorption coefficient, e.g. bleaching of an absorber. A phase grating results from a spatial modulation of the phase of the wave transmitted by the medium and can be produced by changes in pressure, density, temperature, or free carrier concentration altering the propagation velocity in the medium. Such changes are in the real part of the complex index of refraction. When local heating in the sample, with a corresponding

temperature increase, is produced by absorption of energy from the optical beams, unless hydrodynamic equilibrium is maintained, excess pressure is produced in the medium, and an acoustic wave is generated. Thus both a "temperature grating" and an "acoustic grating" can be thermally induced in the medium. Separation and identification of the various mechanisms is possible observing the time behavior and the intensity dependence of the beams generated by the induced diffraction gratings. Optically induced diffraction gratings were observed in such liquid and solid adsorbing media as colored methanol solutions, quinoline, ruby, CdS, ZnO, TiO_2, and adsorbing filters. Cupric sulfate in methanol, and ZnO were studied in detail.

2. Results

A quantitative model for determining the scattered insensitivities was developed based on the wave equation for a stratified media. The solution of the wave equation was expanded into a family of plane wave with each wave propagating at the angle which satisfied Bragg's condition for the periodic structure in the optical properties. A set of equations and solutions for the amplitudes of the plane waves can be found however, closed from solutions are possible for only a limited range of conditions and numerical solutions were obtained for a more general set of grating parameters. Quantitative agreement between the theoretical calculations and the experimental observations was obtained.

Experiments on optically induced scattering in adsorbing media have been carried out. Diffraction gratings were generated in adsorbing media by a change in the optical properties of the medium occurring at the antinodes of an interference pattern.

Several mechanisms for the interaction were identified and correlated with physical properties of the medium. Depending on the material properties, either amplitude or phase diffraction gratings were produced. The theoretical interpretation of the observed scattering compared well with the experimental results.

Mechanisms studied for the interaction were saturation, absorptive heating, and "two-photon" absorption. In the linear absorbers, only absorptive heating was active in the generation of diffraction gratings. This heating produced phase gratings identifiable with changes in pressure or temperature. Saturable absorbers were studies where both saturation and absorptive heating were effective in producing diffraction gratings. Amplitude gratings produced in saturable absorbers were accompanied by a thermally induced phase grating similar to the type observed in linear absorbers.

In a study of grating resulting from electrons, free carriers used to change the index of refraction in two ways. Initially the free carriers contributed a small modulation to the real part of the index of refraction, and later, the recombination through nonradiative cesium produced heating and a temperature induced phase grating.

Optically induced diffraction gratings can be efficient in scattering the incident radiation and is generating additional beams. Scattering was observed at both 6943 Å (ruby laser) and the argon laser wavelengths and scattering efficiencies approached the maximum theoretical values. For a phase grating, the theoretical maximum efficiencies varies from 30% to 100% depending on

grating parameters. These values are representative of the efficiencies observed.

IV. Personnel

A. Professors

R. J. Collins, Director

A. J. Carruthers

A. van der Ziel

W. T. Peria

K. van Vliet

B. Associate Professors

H. Risken

J. Park

C. Assistant Professors

C. Y. She

R. A. Phillips

J. Freudenthal

B. Hocker

R. Weber

V. Theses Published

A. Students who received major support

Bickel, Gary Wayne (Physics - 1974), Ph.D. Thesis: A Study of the Nonlinear Optical Properties of Proustite

Chen, Tzeng Shing (1971), Ph.D. Thesis: A Study of Self-locking of Lasers

Chow, Christopher (Physics - 1974), Ph.D. Thesis: Self-pulsing in Medium Power He-Ne Lasers

Davis, Donald (1970), Ph.D. Thesis: Studies of the Ruby Ring Laser

Dean, David Roy (1971), Ph.D. Thesis: Optically Induced Diffraction Gratings in Liquids and Solids

Franzen, Douglas L. (1970), Ph.D. Thesis: Parameters Affecting the Performance of Carbon Dioxide Lasers and Amplifiers

Lee, Sang Joon (1972), Ph.D. Thesis: Experiments in Superheterodyne Mixing at 10.6 Microns

Nummedal, Kjell (1968), Ph.D. Thesis: Pulse Formation in Lasers

Rayside, John S. (Physics - 1973), Ph.D. Thesis: The Raman Spectrum of Signal Crystal Proustite

Rusch, Thomas (1973), Ph.D. Thesis: An Investigation of Ag-O-Cs Photoemissive Surfaces Using Auger Electron Spectroscopy

Sharma, Raghu (1969), Ph.D. Thesis: Fluctuation Studies in Mercury Cadmium Telluride

Willenbring, Gerald (1973), Ph.D. Thesis: Self-Mode-Locking in Inhomogeneously-Broadened CW Lasers

Hui, Tit kwan (1975), M.S. Paper: An Investigation of the Recombination Processes in ZnO with the Method of Optically Induced Gratings and Photoluminescence

Patrek, William (1971), M.S. Paper: Properties of Transversely Excited CO_2 Lasers

B. Students who received partial support

Abdel, Rahman Mona (1972), Ph.D. Thesis: Hot Electron Effects in SCL Diodes and Mosfets

Anderson, Leroy H. (1969), Ph.D. Thesis: Fluctuation Phenomena in Gallium Arsenide

Chern, Mao-jin (1972), Ph.D. Thesis: A Study of Optical Activity and Raman Scattering in the Sodium Nitrate Crystals

Cunningham, Earl (1970), Ph.D. Thesis: High Sensitivity Measurements of Plasma Dispersion and Parametric Gain at 6328 Å

Hedin, George (1970), Ph.D. Thesis: Adaptive Nonparametrics Reception of Weak Signals in Unknown Nonstationary Environments

Janssen, Raymond (1970), Ph.D. Thesis: An Experimental Approach to Dynamic Characterization of some System Response Statistics

Langseth, Rollin (1968), Ph.D. Thesis: An Adaptive Approach to Receiving Array Optimization Using Stochastic Approximation

Shen, Shu Wei (1972), Ph.D. Thesis: Study of Flux-flow Noise in Type II Superconductors

Zagalsky, Nelson (1975), Ph.D. Thesis: Aircraft Energy Management

Larson, William (1969), M.S. Paper: A Microwave System for the Detection of Photoconductivity and Generation-Recombination Noise, with some Measurements on Cadmium Sulphide

Shen, Shu Wei (1968), M.S. Paper: Noise Suppression in Field Emission